Mechanobiology of Short DNA Molecules: A Single Molecule Perspective

by

Krishnan Raghunathan

A dissertation submitted in partial fulfillment
of the requirements for the degree of
Doctor of Philosophy
(Biophysics)
in The University of Michigan
2012

Doctoral Committee:

Professor Jens-Christian Meiners, Chair
Professor Noel C Perkins
Associate Professor Jennifer Ogilvie
Associate Professor Michal R Zochowski
Assistant Professor Ajit Prakash Joglekar

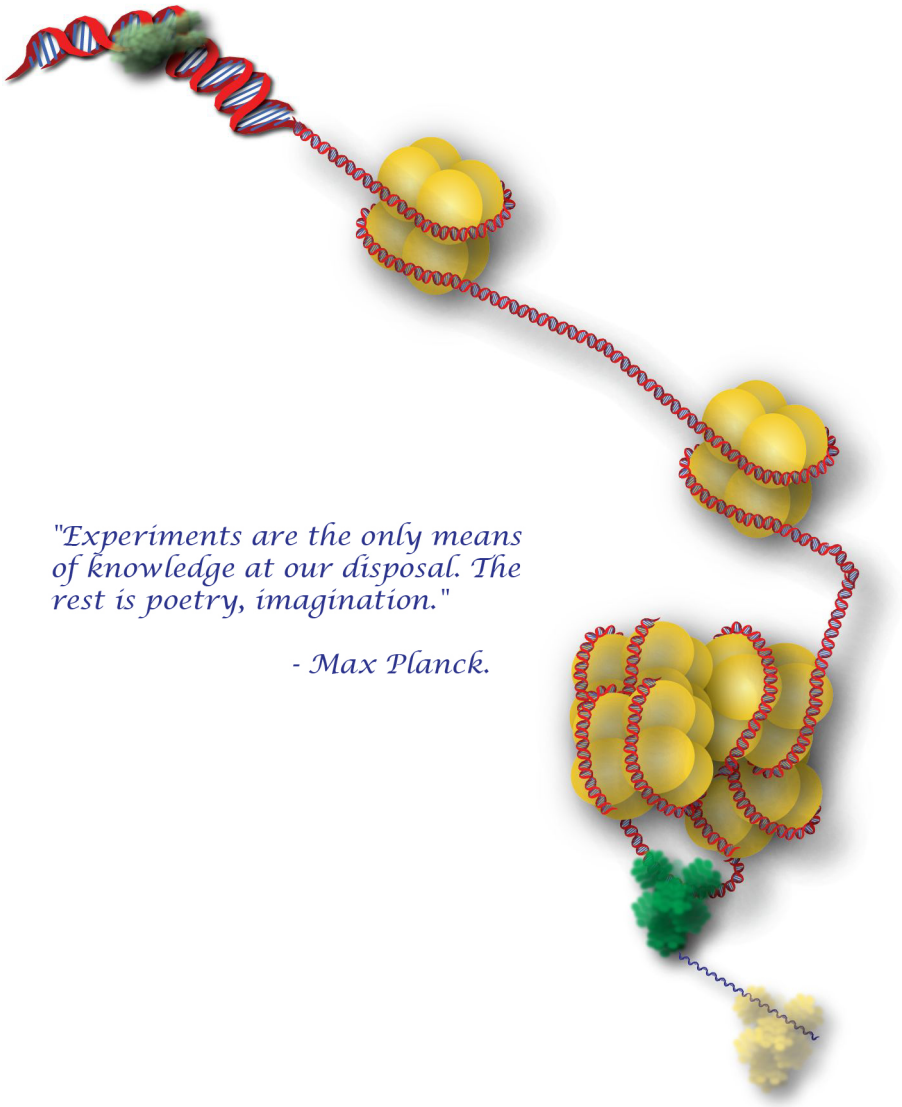

"Experiments are the only means of knowledge at our disposal. The rest is poetry, imagination."

- Max Planck.

परिभ्रमसि किं व्यर्थं क्वचन चित्त विश्राम्यतां
स्वयं भवति यद्यथा तत्तथा नान्यथा।
अतीतमपि न स्मरन्नपि च भाव्यसङ्कल्पय-
न्नतर्कितगमनाननुभवस्व भोगानिह॥

Louise: 'How did you get here?'

Johnny: 'Well, basically, there was this little dot, right? And the dot went bang and the bang expanded. Energy formed into matter, matter cooled, matter lived, the amoeba to fish, to fish to fowl, to fowl to frog, to frog to mammal, the mammal to monkey, to monkey to man, amo amas amat, quid pro quo, memento mori, ad infinitum, sprinkle on a little bit of grated cheese and leave under the grill till Doomsday.'

ACKNOWLEDGEMENTS

Every year 30,000 or so young budding scientists acquire a prefix of Dr. to their name. However, unlike any other degree, each one of us is uniquely molded based on our own experiences, our background, our mentors, amongst other things. It is a metamorphosis much like a chrysalis turning into butterfly. My journey wading through the eventful waters of graduate life reflects more the strengths of people surrounding me more than my own personal ability. Several people have helped me both professionally and personally providing me with sustenance through these years.

I guess I should start with Chris, my 'boss'. It was in my second semester at Michigan when I took Chris's class on Dynamics of Biomolecules that I really became fascinated with polymers and DNA. His back of the envelope calculations and fascination for understanding the physical basis of biological functions rubbed off on me and at the end of the semester I started working in the sub-basements of Randall. Chris has always been the right mentor for me. Many a time, he has gone out of his way to help me. Even when he is cooking for the group, he would make sure to have enough vegetarian dishes for me. On any given time, his doors were always open for his students and he never once expressed frustration at my idiosyncrasies. He is and will always be an inspiration to me.

I should also acknowledge the contributions of rest of my committee members. Jennifer was one of the persons who was responsible for me being in Michigan. Right from my first rotation till today, she has helped me on numerous occasions. Michal taught me a course in Complexity which really influenced me. I will always remember

his patience every time when I always walk into his office with a 'Hi Michal, I need a favor.' Ajit's passion and keen biological insights were very helpful in getting directionality with respect to the second part of the thesis. I hope to follow some of the tips on bacterial strains when we work on the transformation of hairpins into E. *coli* and I thank him for showing much interest in my work. Noel has unknowingly played a greater part in shaping my thesis than he actually realized. It was continuation of the work of his graduate student, Sachin Goyal which forms the basis of the first part of my thesis. His inputs on differences in measurement of persistence length between tweezers experiments and ligation experiments were very useful. Apart from my committee members, I should also thank the Gafni/Steel lab for the photobleaching experiments. One more faculty whom I should thank, Dr. Kristen Verhey in whose lab I learnt all my rudimentary biochemical skills.

I am really lucky to have great labmates, nah, friends, who helped me a lot during my graduate life. Gerhard, who with all his antics and swift puns was not only influential in getting me to join the lab but also made lab so much more fun. He and Kat also helped me in getting started with my work and helped me with many of my initial experiments (things which, alas will never see daylight !!). I should also thank Hao for showing me how to build microfluidic chips. My partner in crime in the lab was Yih-Fan. He helped me with everything, be it giving a ride home or by building the optical tweezers setup which I used for measurement of elasticity. He was an ideal peer to have and I am really happy to have such a good friend. And then, there was this string theorist in lab who was my constant motivator, friend and philosopher. Be it, random Daily Show moments or what the J stood for in J-factor, David is always a fun to talk to. I learnt to stay positive in life from him. He and Margaret are an incredible couple to have as friends. I should further thank David for helping me in understanding the theoretical aspects of my work which would have otherwise been dark to me. I should also thank him as he is one of the handful of

people who actually read my thesis completely (Thanks for the detailed comments too !!). I can very frankly say without Josh, I will still be wandering in the desert, without a goal in sight. His perceptiveness has helped me develop as a researcher and I really learnt a lot from him. Very specifically, I learnt to prioritize what to work on. He contributed quite significantly to all the projects described in the thesis. I should also thank Joel for being helpful with regards to all the TPM. His cheerfulness always made lab a happier place.

There is another body of people that I am especially grateful to, the undergraduates in our lab. These guys are really special and have been invaluable for all of my work. Mike Chu with his deft hands and really amazing patience, provided the basis for many figures in the thesis. He worked on the Dicty project and was responsible for kick starting it. Justin worked on TPM project and was also responsible for maintaining the Dicty culture. Alan is currently working with me on TPM of elastic sequences and contributed for many of the plots that are seen in chapter 4. Ben worked with me on cyclization projects which did not materialize and is currently working on constructing DNA hairpins.

I should thank everyone over at Biophysics for providing me support (both financial and otherwise) over the years. Everyone there, Ann, Sara, Scott and Theresa have always been very helpful. I am equally grateful to the physics department, my second home, and everyone there from Joe to Nicolle and Sherry have helped me a lot over the years. None of my research would have been possible without funding from NIH, NSF and the Focus center. I should further acknowledge financial support from MCDB department and Dr. Shantha for the GSI position.

I should also thank Chamaree, Akash, Liz and Raghu for helping me make Ann Arbor home. Chamaree will always remain a very special friend. And, then there is the junta from back home. All the Indian 'gumbal' Janani, Vikram, Sethu (my roommie), Visa, Kau, K3, Jessie, Diwa, Nisha, Vidyut, KD and Divya. My, what to

say... Thanks guys, none of this would have happened without the love you showered on me and for making me feel so much at home. These few years have been the most wonderful and one of the most important reasons for the same is your company. Everytime we get together, I have always had so much fun. I should thank Kau (who along with Pavi and I) came up with the thesis title. I should thank Vik/Janani for listening and commenting on my research. I should also thank my parents and my sister for their affection and constant support. They have been with me through my success and failure all through my life and have always had faith in me. They have helped me financially, personally and in every other way possible. Finally, I should thank the most important person in my life, my fiancée, Pavi without whose support and love, none of this would have been possible. She was always helping me with different things, encouraging me whenever I was down, critqueing me whenever I needed an introspection and always lending me a shoulder whenver I needed. Professionally, she was the initiator for the numerous scientific coversations we have had over the years and her perspective has always been useful. She also helped me with the photobleaching experiments detailed in chapter 6. I am really thankful for your friendship and for the courage that you have given me and I am really looking forward to spending the rest of our lives together.

I may have missed some people and I should apologize for the oversight.

Krishnan Raghunathan

TABLE OF CONTENTS

LIST OF FIGURES

Figure

LIST OF TABLES

Table

LIST OF APPENDICES

Appendix

ABSTRACT

Mechanobiology of Short DNA Molecules:
A Single Molecule Perspective

by

Krishnan Raghunathan

Chair: Jens-Christian Meiners

Mechanical properties of DNA are known to play a significant role in several biological processes like wrapping of DNA around histones and looping. Most of these cellular events occur on a DNA length scale of a few hundred basepairs. Single molecule methods have been highly successful in directly investigating heterogeneity in different biomolecular systems and serve as ideal tools to study the mechanical properties of DNA. However, their use in studying DNA of contour lengths less than a kilobase are fraught with experimental difficulties.

The research presented in this thesis explores the behavior of short stretches of DNA ($\leq$ 500bp) using existing and novel single molecule methods. We have quantified the variation in persistence lengths between sequences having different elasticity using a constant force axial optical tweezers. Our experiments have also revealed that this difference in persistence lengths manifests itself as a difference in looping lifetimes of lac repressor, in sequences having the aforementioned constructs as the intervening sequence between the operator sites. We have also developed a system to probe DNA dynamics *in vivo*. We have found that the active processes in the cell have

distinct effects on dynamics of DNA and eliminating the active processes causes a 'phase transition' like behavior in the inside the cell. We are currently extending this technique to understand DNA dynamics inside bacterial systems. Our results provide vital insights into mechanical properties of DNA and the effect of athermal fluctuations on DNA dynamics.

CHAPTER I

Introduction

1.1 DNA-101

In 1953, James Watson and Francis Crick at the Cavendish Laboratory, Cambridge elucidated the intrinsic structure of DNA using data from Rosalind Franklin [*Maddox* (2003)]. The simple, yet elegant, double helical structure of the DNA has ever since captured the imagination of both the scientific and the non-scientific community [*Watson* (2011)]. Ironically, the very structure of DNA which established its place as the molecule that encodes the entire blueprint of an organism, also showcased its inertness. Further, biochemical discoveries in the subsequent decades following this, firmly established proteins as the main workhorses of the cell [*Strong and Eisenberg* (2007)]. The unintended consequence of this was that the regulatory role played by the structure of DNA was relegated to the backbenches of research [*James K* (1997)]. However, DNA itself was not lost from research, with several spectacular discoveries based on DNA from sequencing the human genome [*Lander et al.* (2001); *Venter et al.* (2001)], solving the traveling salesman problem [*Adleman* (1994)] to a fancy molecular cartoon of the world map [*Rothemund* (2006)] being few of the landmark papers featuring DNA over the years. However, DNA itself continued to be viewed as a passive molecule not directly influencing any biochemical function.

1.2 DNA-Protein Interactions

Besides, the more famous life of DNA as an information carrier, it is also known to act as a binding substrate for several proteins in a variety of manner. Simplest case of this are proteins recognize and bind to a unique sequence of DNA. The classic example of these is the TATA box binding protein which binds specifically to the DNA sequence TATAAT to initiate transcription. Other examples include transcription factors, enhancers, specific restriction endonucleases and repressors. A ubiquitous theme that is seen in many of the regulatory events and one that be referred extensively in this thesis, is the ability of two distal ends of DNA to come close and be bound by a protein complex to form a DNA loop. A canonical example for the same is the lac repressor loop where the repressor tetramer recognizes two short 20bp sequence of DNA that are separated by a longer stretch of DNA. A second class of DNA binding proteins do not have any specific recognition sequence. An oft quoted example is the wrapping of DNA around histones enabling compaction of the genome. Typically around 150bp of DNA wraps around a histone in about 1.7 turns to form a nucleosomal complex with around 50bp linker DNA between adjacent nucleosomes. The final class of proteins are those that bind and act non-specifically with DNA as transient substrates. Common examples include polymerases, topoisomerases and helicases. These enzymes not only catalyze reactions but also impact mechanics of DNA directly. The question arises as to whether in all these interactions, the DNA behaves as a passive substrate or if it actively regulates these biological processes.

1.3 Mechanics of Short DNA Sequences

In the past decade, there has been growing interest in how these different protein-DNA complexes respond to various mechanical/thermal forces. A more exhaustive list of mechanical properties known to affect DNA-protein complexes is given in figure

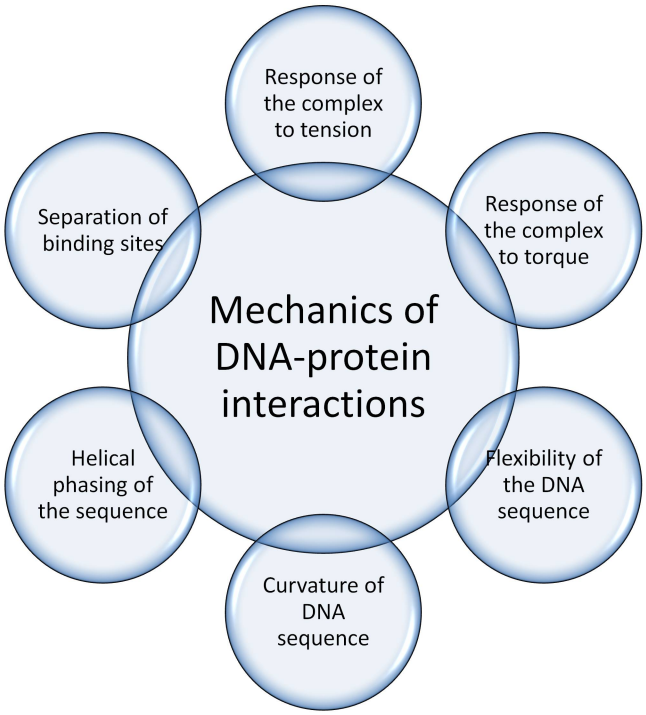

Figure 1.1: **Different Mechanical Properties Affecting DNA-Protein Interaction** Many physical properties of DNA are known to influence DNA-protein interactions. A few of these are given in the figure Adapted from Seth Blumberg [*Blumberg* (2006)]

1.1. It is known that by modulating these mechanical properties, DNA can make itself better amenable to genetic regulation.

In a series of classic experiments by Muller Hill [*Kraemer et al.* (1988, 1987); *Lehming et al.* (1987)], length of DNA and helical repeat in the inter-operator region between the lac operators was varied and the gene repression was found to be linked to physical properties of the non-binding interoperator DNA. For instance, the helical phasing of the DNA directly correlated with the level of repression up to a loop length of $\approx$ 300bp. These results along with development of a then novel biochemical technique, ring cyclization [*Shore et al.* (1981); *Kahn et al.* (1994); *Kahn and Crothers* (1992)] spurred active research into studying the mechanical properties of short DNA constructs. Further interest in the field was piqued when the late Jonathan Widom

discovered underlying signatures in the DNA bound to nucleosome [*Segal et al.* (2006)] showing that DNA does not randomly bind to the histones, and certain sequences are preferentially positioned for nucleosomal binding. Introduction of these signature motifs into any sequence is currently postulated to affect the flexibility of DNA [*Garcia et al.* (2007)]. Further work by Widom has shown that short DNA molecules are inherently more flexible [*Cloutier and Widom* (2004, 2005)] than what was previously thought, although new findings have disputed such claims [*Du et al.* (2005)]. It is becoming increasingly evident that mechanics of short DNA molecules can affect biological functions significantly. Currently, there is an increasing number of attempts to further understand the biological implication of DNA mechanics and to quantitatively describe the mechanics of DNA. My thesis follows along similar lines and aims to quantitate sequence dependent effects on DNA elasticity and to understand the biological implications of such effects.

1.4 Hurdles in the Path: Bypassing the Mines of Moria

There are three important factors that are to be carefully addressed whilst understanding the importance of mechanics in biology. They are

1. Delineating the physical property of interest without changing other mechanical properties.

2. Using the appropriate experiments for studying the system of interest

3. Using experimental results to understand the property of interest using proper theoretical framework

Each of these will be elaborated in the subsequent paragraphs with regards to the system I have studied.

1.4.1 Two Sides of the Ring: Curvature and Elasticity

Mechanics of DNA is an umbrella term used to describe several physical parameters of DNA, each of which though unique, is inherently dependent on the sequence of the DNA strand [*Travers and Thompson* (2004)]. For instance, changing the number of bases between two operator sites not only changes the length of DNA, but might also vary the helical phasing of DNA. The implication of this interdependence is that difference in looping lifetimes between say two sequences, one which is 90bp and other that is 91bp should not only account for the difference caused by addition of the base but also the angular difference between the distal ends as they come close. Similarly, for a given length of DNA, variation in its sequence affects bendability and changes its curvature. Sequence bendability and curvature are thus two interrelated physical properties. In this thesis, we are interested in understanding how specific changes to the sequence of DNA uniquely affect the elastcity of DNA and consequently biological function. Curvature of DNA is the intrinsic anisotropic bend adopted by the molecule and is even present at absolute zero [*Goodsell and Dickerson* (1994)]. Curvature in DNA originates from the deviation from average stacking that occurs in a random nucleotide sequence due to introduction of certain sequence repeats. Elasticity of DNA on the other hand is a more subtle physical property which describes the ability of DNA to respond to force. At any temperature greater than absolute zero, thermal fluctuations influences the way DNA stays coiled. By applying an external force, it is possible to entropically extend the DNA. This response determines the elasticity of DNA. For instance, it is conceiveable to have a rubber band and a circular steel rod having the same circumference. However, upon application of a force, the rubber band responds differently compared to the steel rod. However unlike rubber and steel, delineating one property from another in case of DNA is not trivial as varying the sequence changes both these physical properties [*Goyal et al.* (2008)]. For instance, an A tract bend is not only prebent but can also be more flexible. *So any attempt to*

isolate the biological implication of bendability of DNA should avoid any interference of curvature in the system.

1.4.2 Rise of the Machines

Over the past two decades, several single molecule and force measurement methodologies have been developed for studying many biological systems. These single molecule methods have an inherent advantage over traditional biochemical experiments as they are more sensitive to heterogeneities in the system as opposed to the ensemble averaged measurements [*Strick et al.* (2000)]. Novel biophysical tools including Atomic Force Microscopy [*Marilley et al.* (2005)], sm-FRET [*Morgan et al.* (2005)], optical tweezers [*Koch et al.* (2002)] and magnetic tweezers [*Lia et al.* (2003)] have been used to study various nucleic acid systems. However, traditional tweezers experiments operate in the realm greater than a couple of kilobases and imaging techniques like sm-FRET cannot be used effectively for length scales greater than a couple of tens of bases. This limits the questions that can be completely addressed without further supporting biochemical experiments. *Thus, it becomes imperative to develop a single molecule methodology which can be used for the length scales relevant to the biological problem, in this case, a few hundred bases.*

1.4.3 From Basepairs to Polymer

To really understand an experimental result, it becomes imperative to have a strong theoretical framework. As we go from studying properties of short lengths of DNA within a helical repeat to much larger length scales, the atomistic description of the DNA sequence becomes an overkill [*Becker and Everaers* (2007)]. In longer length scales, the DNA is better described physically as a polymer and can be described by several physical models with the Worm-Like Chain (WLC), where the DNA is described as a continuous semiflexible polymer, being the most used description [*Doi*

and Edwards (1988); *Marko and Siggia* (1995a)].

The parameter that describes the intrinsic stiffness of a polymer is called persistence length(l_p). Consider theroretically we are moving along the backbone of the DNA, the change in tangent vector along the backbone falls exponentially over a characterstic length. This characterstic length scale is called as the persistence length. Persistence length is a macroscopic manifestation of a microscopic phenomena. Stretching DNA upon application of force enables in precise measurement of persistence length. It has been shown that the entropic extension of the DNA on application of an external force can be modeled fairly accurately using the WLC model [*Bouchiat et al.* (1999)]. Typically, the persistence length for a long unbiased DNA, *in vitro*, is roughly 50 nm and roughly translates to 150bp [*Bouchiat et al.* (1999)]. The physical implication of this is that DNA less than the persistence length is rod like and in length scales much greater than this is flexible. However, in short length scales, it is possible to bias the sequence to exhibit unique behavior having functional significance and on short length scales, the boundary conditions for describing the DNA becomes important. The WLC model needs to be modified to accommodate these and the very concept of the persistence length needs to be revisited.

Tom Perkins modified the WLC model into an entirely new model, to accommodate boundary condition effects [*Seol et al.* (2007)]. Alternatively, it was also proposed that it is possible to modify the existing WLC model by introducing a correction factor to l_p. This correction is dependent on the DNA contour length in contrast to the length invariant traditional persistence length (henceforth referred to as **nominal persistence length**). When the correction is added to the nominal persistence length, the resulting length-dependent **effective persistence length (l_p^*)** subsumes all boundary corrections into a singular parameter. In our previous work, we have proven experimentally that the l_p^* allows the classic WLC model to be used with DNA as short as 250bp [*Chen et al.* (2009b)]. Interestingly, the effective persistence

length decreases to nearly half the value of nominal persistence length for extremely short DNA lengths. In our experiments, this modified WLC model will be used to determine persistence length of DNA and this measure of persistence length will be used as the parameter for measuring stiffness.

1.4.4 Outline of Research - Chapters 2-4

The first part of my thesis aims to describe quantitatively sequence dependent effects on a physical property of DNA, its bendability and how sequence elasticity influences a biological event, namely looping rates.

System to study mechanics of short DNA molecules

Chapter 2 describes the construction and usage of a constant force optical tweezers. This methodology developed in our lab is ideal for stretching short DNA molecules. We have successfully used these tweezers for stretching DNA as short as 250bp. This chapter describes construction, alignment and calibration of the tweezers.

Quantifying the effect of sequence variation on elasticity of DNA

Chapter 3 describes how sequence variation can modulate the elasticity of DNA. We have successfully implemented a methodology described in this chapter to delineate sequence elasticity from curvature. We have determined persistence length of these constructs. Our principal finding is that persistence length varies by almost 30% when AT content changed by 15%.

Understanding how the biological relevance of the sequence variation

Chapter 4 describes looping experiments using the aforementioned sequences. Using lac operator on either ends of sequences with varying elasticity, we have carried out Tethered Particle Motion experiments. These experiments reveal how the difference in persistence length manifests itself as lifetime of (un)looped

states.

1.5 Cellular Environment and DNA

Neglected in the first part of the thesis is an important factor in understanding any biological function, the influence of the discombobulated mess of the cellular environment [*Norris and Malys* (2011)]. The native environment of the any biochemical reaction is the highly crowded, highly fluctuating microenvironment [*Maheshri and OShea* (2007)]. In his classic commentary, the Nobel Laureate, Arthur Kornberg [*Kornberg* (2000)] very presciently said

> '... that some of their (enzyme's) functions, individually and collectively, can be observed despite great dilution is a fortunate break for biochemistry.'

While the statement does not still capture the entire dynamics of the cell, it paved the way for thinking about the microenvironment of the cell. Many studies have since studied the effect of environment on biological reactions. For instance, it is known that a force of 20pN can completely stop RNA polymerase machinery [*Wang et al.* (1998)], a force which can be generated purely by environmental factors, as it is known that force generated by individual motor proteins can reach 10pN [*Brangwynne et al.* (2007)]. It is further known that crowding can be coupled to the biomolecule of interest [*Zhou et al.* (2009)]. For instance, to study looping inside a eukaryotic cell, we need to not only consider all the mechanical properties as previously described, but also the influence of additional factors [*Shin and Sung* (2012)] such as tension generated by proteins such as RNA/DNA polymerases, increased thermal noise due to the four hundred or so fold increased density of particles (compared to aqueous environment), non-competitive interactions with other biological processes that also occur in the vicinity of the region [*MacKintosh and Schmidt* (2010); *Mizuno et al.* (2007)].

Further, *in vivo*, biological processes can be approximated to be in equilibrium only in extremely short time scales (milliseconds), as beyond that due to effects such as remodeling of cytoskeleton, almost all biological processes exist out of equilibrium [*Brangwynne et al.* (2009)]. Thus, to truly comprehend the entire spectrum of any biological event, it is exigent to understand role of the cellular environment.

Several studies have shown the importance of understanding of these environmental effects in biological functionality [*Grima* (2010)]. For instance, rate at which restriction enzyme ECORV catalyzes DNA breakages is dependent on tension while BamHI works independently [*Skinner et al.* (2011)]. Previous work from our lab has shown that few hundred femtonewtons of force can stop DNA loops from forming [*Chen et al.* (2010a)]. Individual histones need only a few piconewtons to dissociate from DNA [*Kruithof et al.* (2009)]. Kornberg's own experiments showed that oriC replication needed a crowded environment for the enzymes to work [*Fuller et al.* (1981)]. It has been shown that diffusion constant of DNA falls dramatically when the length of a DNA probe increases to greater than 250bp and actin cytoskeleton is the component responsible for this [*Dauty and Verkman* (2005)].

However, a complete investigation into the environmental effects hit a brickwall as most experimental techniques are completely unsuitable for directly looking at dynamics of single molecules inside cells [*Milstein and Meiners* (2011)]. Most information on the mechanical properties' modulation of function inside the cell come from biochemical experiments that look at bulk properties or from fluorescent techniques, which make use of the family of fluorescent proteins [*Baumann et al.* (2010)]. Again, because of diffraction limits and other practical difficulties such as high fluorescent background, it becomes difficult to look at single molecule dynamics *in vivo*. With the advent of super resolution microscopy, some aspects of protein/lipid dynamics inside a cell is currently being studied [*Sengupta et al.* (2011)]. However, no experimental techniques have been developed to study real time DNA loop formation and

breakdown inside a cell.

1.5.1 Outline of Research - Chapters 5-6

The final two chapters of my thesis describe experiments that can be used to study cellular events that are quite difficult to observe, if not wholly inaccessible to existing single-molecule techniques.

Dynamics inside Dictyostelium *discoideum*

Chapter 5 describes our experimental system that can be used to follow looping inside a living cell. The chapter further explores how dynamics of DNA changes upon removal of active processes. We hypothesize that active forces remodel the cellular environment and their absence results in a 'glass phase transition'.

DNA in Bacteria

We are currently modifying our experimental system to make it amenable for use in bacterial system. Bacterial systems are inherently simpler to handle and provide a more relevant environment for following lac loop formation. We have shown that it is possible to synthesize dually colored, multiply labeled strands of DNA. This work will be expanded to follow dynamics inside of bacterial cell. These experiments will be complementary to the experiments using FCS that are also simultaneously being carried out in our lab to understand the effect of active processes in nucleic acid dynamics *in vivo*.

CHAPTER II

'..Just around the Corner, till the Light of Day: Using Optical Traps to Study Short DNA Molecules'

2.1 Introduction

Single-molecule techniques for stretching DNA of contour lengths less than a kilobase are fraught with experimental difficulties. However, it is in this submicron regime that many interesting biological events such as histone binding and protein-mediated looping of DNA [*Halford et al.* (2004); *Allemand et al.* (2006)] occur. In recent years, the mechanical properties of DNA have been shown to play a significant role in fundamental cellular processes like the packaging of DNA into compact nucleosomes and chromatin fibers [*Kaplan et al.* (2008); *Garcia et al.* (2007)]. Clearly, it is then important to understand the mechanical properties of short stretches of DNA. In this chapter, we provide a practical guide to a single-molecule optical tweezing technique that we have developed to study the mechanical behavior of DNA with contour lengths as short as a few hundred basepairs.

The major hurdle in stretching short segments of DNA is that conventional optical tweezers are generally designed to apply force in a direction lateral to the stage [*Neuman and Block* (2004); *Moffitt et al.* (2008)] (see Figure 2.1) and in this geometry,

the angle between the bead and the coverslip, to which the DNA is tethered, becomes very steep for submicron length DNA. The axial position must now be accounted for, which can be a challenge, and, since the extension drags the microsphere closer to the coverslip, steric effects are enhanced. Furthermore, the microspheres are asymmetric and lateral extensions will generate varying levels of torque due to rotation of the microsphere within the optical trap since the direction of the reactive force changes during the extension.

Alternate methods for stretching submicron DNA run up against their own unique hurdles. For instance, a dual-beam optical trap is limited to stretching DNA of around a wavelength, at which point interference effects between the two traps and from light scattering between the microspheres begin to pose a significant problem. Replacing one of the traps with a micropipette would most likely suffer from similar challenges. While one could directly use the axial potential to stretch the DNA, an active feedback scheme would be needed to apply a constant force and the bandwidth of this will be quite limited, especially at low forces.

We circumvent these fundamental problems by directly pulling the DNA away from the coverslip by using a constant force axial optical tweezers [*Chen et al.* (2009a,b)]. This is achieved by trapping the bead in a linear region of the optical potential, where the optical force is constant-the strength of which can be tuned by adjusting the laser power. Trapping within the linear region also serves as an all optical force-clamp on the DNA that extends for nearly 350 nm in the axial direction. We simultaneously compensate for thermal and mechanical drift by finely adjusting the position of the stage so that a reference microsphere stuck to the coverslip remains at the same position and focus, allowing for a virtually limitless observation period.

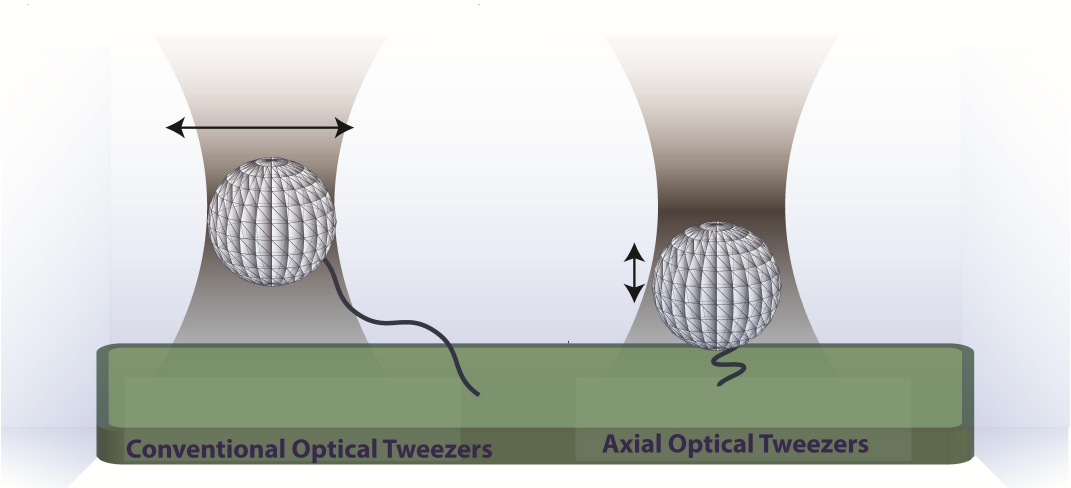

Figure 2.1: **Principle of Axial Optical Tweezers:** (Left) Conventional optical tweezers trap near the focus. The bead is then moved lateral to the coverslip to exert tension. (Right) In axial optical tweezers, a microsphere is trapped away from the focus, in the linear region of the optical potential. In this configuration, the polymer is held under constant tension for a range of extensions. Moreover, increasing the laser intensity moves the microsphere in the axial direction

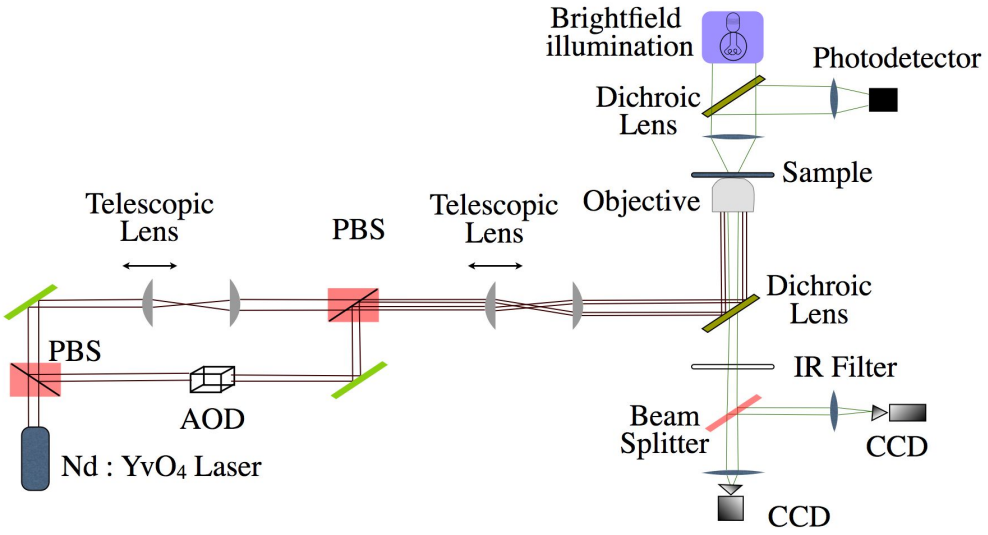

Figure 2.2: **Schematic Representation of Axial Optical Tweezers:** Laser light (1064nm Nd:YvO4) is split into two beams by passing through a polarizing beam splitter (PBS) from which one, the manipulation beam, passes through an acousto-optical deflector (AOD) while the other, the calibration beam, can be adjusted independently using telescopic lenses. The two beams are then recombined using another PBS, reflected by a dichroic lens and focused onto the sample by a high N.A. objective. Simultaneously, brightfield illumination, used to track the microsphere, passes through the sample, is Infra Red (IR) filtered and is then imaged by two CCD cameras, one of which takes measurements while the other acts as part of a feedback control system.

2.2 Tweezers Setup

1. The beam from a 1064 nm laser is split into two orthogonally polarized beams. One is used to manipulate the biomolecule while the other is used for calibration purposes (see Figure 2.2).

2. The intensity of the manipulation beam is controlled by an acousto-optic deflector (AOD), while the position and focus of each beam is independently controlled by beam steering mirrors and optical telescopes, respectively.

3. The beams are then recombined with another polarizing beam splitter and

conditioned further by a final set of telescoping optics to slightly overfill the back aperture of the microscope objective. A 50% overfill for the calibration beam leads to a tight optical trap, while a slightly smaller factor for the manipulation beam, approximately 20%, gives a shallower focus that translates into a larger workable region of the linear potential. Finally, the beams are tightly focused by with a PlanApo 60x/1.4 oil immersion microscope objective onto the sample cell.

4. This tweezers setup is combined with a home built brightfield microscope that provides illumination from a Halogen lamp focused onto the sample chamber by a condenser. The brightfield image is separated from the laser light by a dichroic mirror and then imaged on two CCD cameras. One CCD acts as our primary means of acquiring data and is software triggered to yield precise sampling rates, while the other CCD is used to image a single stuck reference microsphere whose position serves as part of a feedback-control system that compensate for drift in the microscope. compensate for drift in the microscope.

5. The sample is coarsely positioned with respect to the objective by an XY stage, and can then be precisely positioned by an embedded three dimensional piezo-stage.

6. The forward-scattered and transmitted laser light is collected by the brightfield condenser and focused onto a photodetector. The resulting signal is filtered through an anti-aliasing filter at 100 kHz, amplified and acquired at 200 kHz using a DAQ card.

2.3 Calibrating Apparent Size of the Bead to Axial Position

1. Load a sample chamber [*Document* (2009)] with a disperse solution of 800nm diameter polystyrene microspheres diluted in phosphate buffered saline buffer.

Let sit for 10-15 minutes and then lightly flush with buffer to remove excess microspheres.

2. Locate a microsphere randomly stuck to the coverglass and adjust the height of the sample chamber until the microsphere is approximately 1m below the focus to generate a defocused image.

3. To measure the apparent size of the image, first find the centre of the microsphere using the geometric pattern matching function in LabView.

4. Next, generate a radial intensity profile of the microsphere by averaging 360 about the center of each cross section. The radial profile, which corresponds to a white ring in each of the brightfield images, can be fitted with a quadratic function to find a brightness peak. The distance between this peak and the center can be used as a measure of the apparent size of the bead.

5. Using the calibrated piezostage, gradually increase the axial position of the microsphere and acquire an image at each axial position with the CCD camera an image at each axial position.

6. Repeat the image analysis for each successive image to correlate the apparent size of the microsphere with its axial location (see Figure 2.3). The axial resolution obtained by method is around 1.4 nm [*Chen et al.* (2009a)].

2.4 Mapping Optical Potential of the Manipulation Beam

1. Begin by collinearly aligning the manipulation beam and the calibration beam. The calibration beam should be around 50 mW at the back aperture of the objective while the manipulation beam should be of much weaker, say 10 mW.

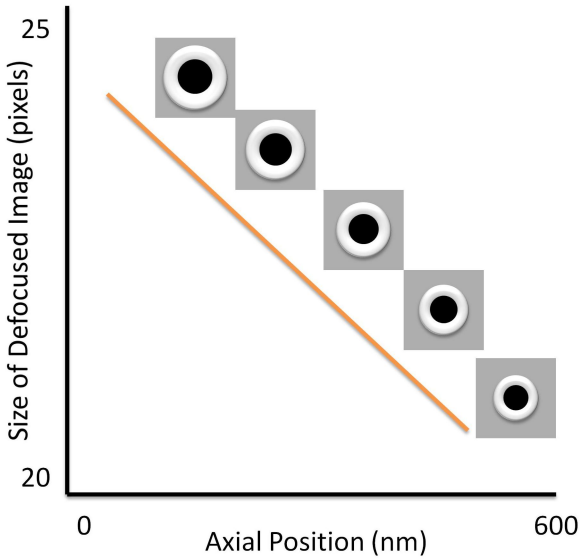

Figure 2.3: **Axial Position Calibration:** To calibrate the axial position, we acquire defocused images of a bead stuck to the chamber coverslip at varying axial positions of the stage. The size of the microsphere is given by the distance between its center and the position of peak intensity about the bright ring formed around the image of the microsphere.

2. With the manipulation beam switched off, confine a free microsphere within the much stiffer trap of the calibration beam.

3. Now, turn on the manipulation beam. Since the manipulation beam is much weaker than the calibration beam, the axial position of the microsphere will be slightly perturbed. The resulting change in axial position can be measured from the defocused brightfield imageimages as already described.

4. Turn off the manipulation beam and, with the microsphere still trapped in the calibration beam, shift the axial focus of the calibration beam by adjusting the telescopic lens. Turn on the manipulation beam and, measure the subsequent displacement of the microsphere and repeat. The displacements ΔX can be plotted against the axial position of the focus of the calibration beam. The axial position corresponding to the largest displacement of the microsphere determines the center of the linear region of the optical trap (see Fig. 4).

5. The final step in obtaining the optical force of the manipulation beam as a function of axial position requires a careful measurement of the stiffness of the calibration beam. To obtain this, move the microsphere, trapped by the calibration beam, to the center of the linear regionaround a micrometer above the surface by adjusting the telescopic lens while the manipulation beam is switched off.

6. Record the thermal axial motion of the microsphere by measuring the intensity of transmitted light with a photodetector.

7. The autocorrelation of the signal can be fitted to a single exponential decay function to give the time constant of the fluctuations, τ_z. The hydrodynamic friction coefficient η, of the microsphere can be corrected for the microspheres proximity to a surface [*Neuman and Block* (2004); *Howard* (1961)]. The stiffness

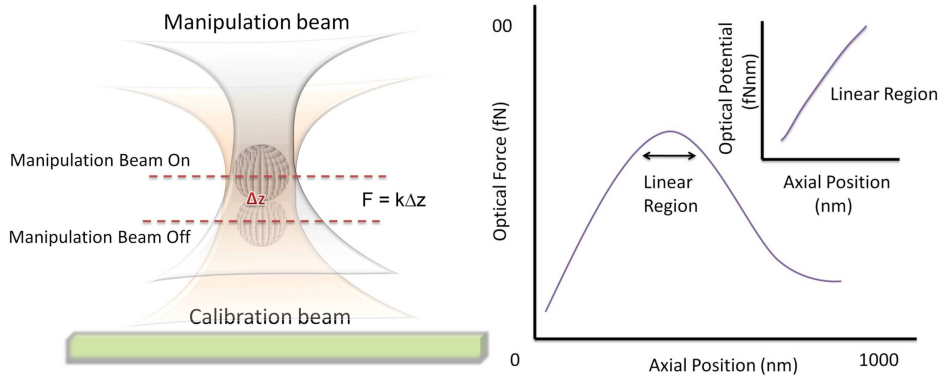

Figure 2.4: **Principal Behind Mapping the Optical Potential:** To map out the optical force of the manipulation beam, one measures the axial displacement that it induces on a microsphere trapped within a much stronger calibration beam. One can locate the center of the linear region where this displacement is a maximum. The Optical Force vs. Axial Position curve can be integrated to find the optical potential.

of the calibration trap is then given by $k_z = \frac{\eta}{\tau_z}$ (see Supplementary Materials A).

8. Knowing the stiffness of the calibration trap allows one to convert the previously measured axial displacements into a force $f_z = -k_z \Delta X$. Integration of this curve yields a spatial mapping of the axial optical potential of the manipulation beam (see Figure 2.4).

2.5 Stretching a DNA sample

1. Mount the chamber containing surface tethered DNA molecules (≤ 1 kbp) and, while observing the brightfield image, place the focus of the manipulation beam slightly above the unstretched microspheres by adjusting the telescope. Then adjust the position of the stage until one of the microspheres gets trapped.

2. Roughly position the microsphere in the center of the XY plane of the optical

trap. Generate a series of square waves can be generated in LabView and send them to the AOD to repetitively turn the laser beam on and off. Carefully control the intensity of the laser and the duration of the on state should be carefully controlled to prevent heating of the sample chamber. Typically, we use around 2 mW of laser power (measured at the back aperture of the objective) and send pulses of 200 ms (on) and 500 ms (off). The amplitude of the square wave sent to the AOD should be around 0.5 V.

3. Watch the microsphere as the trap is repeatedly turned on and off and note if the laser induces any preferential direction to the microsphere's motion. While iteratively adjusting the microsphere position in both the X and Y direction, by controlling the piezostage, the random motion of the microsphere should become isotropic in the XY plane, though noticeably restricted when the laser is on.

4. Next, one should align the bead in the Z direction. Again pulse the laser beam should again be pulsed on and off while, this time, simultaneously measuring the microspheres axial displacement in real time. Center the stage should be centered within the linear region, which is the point where the Z displacement is greatest.

5. After a careful alignment in the Z direction, it is imperative to check that the trap is still centered in the XY plane. If the XY alignment has changed, both the XY and Z alignment must be repeated until the microsphere is centered properly along all three axes.

6. For stretching the DNA, we ramp the laser intensity by sending a voltage signal to the AOD, from 0 V to 0.5 V in steps of 0.025 V. In each step, we record 400 frames at 100 fps and average them to obtain the axial displacement.

7. The force extension curves can now be plotted and fit to a modified WLC model [*Marko and Siggia* (1995b)] (see Supplementary Materials A).

2.6 Representative Results:

We present force extension curves for two DNA sequences: a 1298 bp and a 247 bp sequence, the latter being the shortest sequence we have been able to stretch reproducibly. For short stretches of DNA, the conventional WLC model does not fully explain the force extension relationship because at these length scales as one must account for finite-size effects and zero force extension arising from boundary constraints. The force extension measurements, therefore, have to be fit using a modified WLC model which imbibes in it an effective persistence length and a zero force extension as fit parameters, described further in the supplementary materials. For large contour lengths of dsDNA, the effective persistence length is simply the nominal persistence length (50 nm) and the zero force extension can be neglected. However, as the contour length becomes shorter the effective persistence length decreases well below 50 nm and the DNA, even under zero force, shows a significant extension.

The data and the corresponding fits of the force extension curves are shown in Figure 2.5 for the two sequences. From the modified WLC fits, we have determined the effective persistence lengths to be 35 nm for the 1298 bp DNA and 25 nm for 247 bp DNA. For illustrative purposes, reasons we are presenting single measures of the force extension curves for each sequence. In practice, one would repeat the measurements multiple times and obtain the average results along with the standard errors. It must also be noted that after obtaining each curve it is imperative to ensure that the microsphere remains trapped and properly positioned within the linear region, otherwise the microsphere must be realigned as previously described.

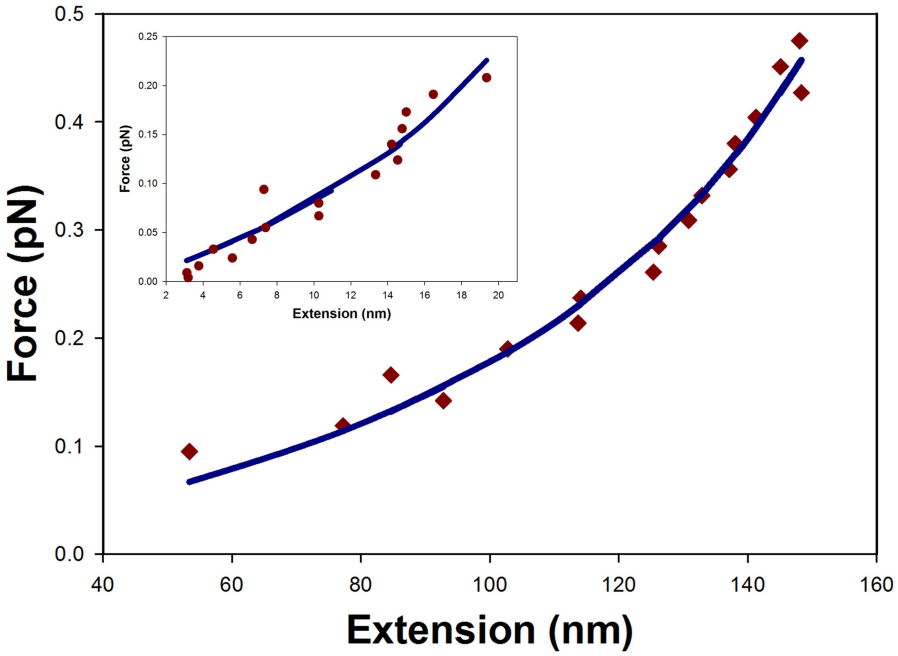

Figure 2.5: **Force Extension Curve:** Data is shown for a random 1298 bp and 247 bp (inset) segment of dsDNA stretched by axial optical tweezers. The data points were fit to the modified WLC model of Eq. 3 (solid lines) and yielded effective persistence lengths of 34 nm and 25 nm, respectively

2.7 Conclusion:

Conventional optical tweezers, in general, rely upon either analog or computer controlled feedback to apply a constant force on a refractile object. These active feedback systems have difficulty performing under conditions where sudden changes in the extension of the specimen occur, for instance, from the binding of a protein to DNA or the rapid stepping of a molecular motor along a filament. Various passive methods for applying constant forces have recently been developed. One such method, used to resolve the stepping of RNA polymerase at basepair resolution, involved working within the linear region of the optical potential of a Gaussian laser beam [*Chen et al.* (2009b)]. We have adapted this method for the manipulation of short biomolecules by creating a constant-force axial optical tweezers.

Axial optical tweezers can be used to study short stretches of DNA that are inaccessible to manipulation by conventional optical methods. They have been used to study the elasticity of short DNA molecules as small as a few hundred base pairs [*Chen et al.* (2009b)] and to probe the effects of elastic tension on protein-mediated DNA loops [*Chen et al.* (2010b,a)]. On short length scales, sequence dependent effects arising from variations in hydrogen bonding and stacking energies, may strongly contribute to the elastic properties of DNA. Axial optical tweezers are an ideal tool for uncovering these sequence dependent effects onto DNA elasticity [*Raghunathan et al.* (2011)]. Moreover, axial optical tweezers would will be a sensitive tool for studying the wrapping of DNA around individual histones or for probing the activity of any rapidly processing molecular motor, and would prove to be a valuable new technique in the single-molecule toolbox.

CHAPTER III

How does Sequence Affect Elasticity ?

3.1 Introduction

In every somatic human cell, there are a roughly two meters of DNA which is packed into a few square micrometers through a series of compactions starting with the wrapping of naked DNA around histones, forming compact chromosomes in the end. The classical view that this nuclear architecture remains static in a cell, has been challenged in the past two decades and there is an increasing amount of biochemical and genetic experiments have revealed the dynamic nature of chromatin [*Widom* (2001)]. While mechanical nature of DNA plays an important role in DNA compaction, it is not an isolated example. The DNA sequence, which gives rise to the mechanical properties of DNA, has been implicated as crucial in transcriptional regulation involving DNA-protein complexes. This form of regulation is particularly seen in both prokaryotes and eukaryotes, where two distal regions on a single DNA strand are looped by a linker protein like Lac repressor [*Chen et al.* (2010a)]. Mechanical constraints affecting the looping kinetics include tension along the DNA backbone, helical alignment of operator sites, supercoiling and stiffness to name a few. In our current work, we intend to understand the effect of sequence on one such mechanical aspects of DNA, its intrinsic bendability.

Deformations in DNA can be traced back to two physical properties of DNA,

namely, curvature and elasticity. These are two related yet distinct properties conferred on DNA by its sequence. While curvature refers to athermal permanent, static bend of DNA like A-tract regions. Elasticity refers to the dynamic bendability of DNA in response to force [*Calladine and Drew* (1986)]. Varying the sequence of DNA can independently change both the curvature and the elasticity.

While many researchers have worked extensively on the effect of curvature on looping and other biological functions of DNA [*DiGabriele and Steitz* (1993); *Morgan et al.* (2005)], understanding the effect of sequence on elasticity of DNA exclusively, has been hindered by the inherent overlap between these two mechanical properties. Importance of short constrained stretches of DNA are highly relevant biologically as DNA of most higher organisms are compacted into subpersistence lengths in histones.

Studying DNA sequences with contour lengths around a persistence length is fraught with difficulties. Many conventional experimental techniques are not suitable for measuring the subtle changes associated with behavior on this short length scale. While theoretical studies using dinucleotide and trinucleotide models have been successfully used to understand the mechanical properties of DNA, quantitative experimental conformation has been lacking in many cases. Furthermore, in some cases, the predictions from different models disagree [*Scipioni et al.* (2002)].

In our earlier work, we successfully developed a constant force axial optical tweezers which can, unlike conventional optical tweezers stretch submicron lengths of DNA [*Chen et al.* (2009a)]. Work in our lab previously used the tweezers to measure the persistence lengths of DNA molecules as short as 247 bp and found that the apparent persistence lengths of DNA shortens with decreasing contour length of the DNA [*Chen et al.* (2009b)].

In this thesis, we describe force extension measurements of three DNA constructs with increasing AT content using constant force axial optical tweezers. The three constructs were designed to have similar curvature but varying elasticity. We found

these sequences to have significantly different persistence lengths. As much as thirty percent difference in the persistence length can arise from a fifteen percent in sequence composition.

3.2 Methods

3.2.1 Sequence Design

We adapted the methodology followed by Goyal et al [*Goyal et al.* (2008)] who designed theoretical sequences to explore sequence dependent effect on cyclization. Our basic constructs are three subpersistence length (132bp) DNA sequences with varying AT content, but having similar curvature as verified by subsequent theoretical and experimental work. The design of sequences for other experiments were based on the motifs designed above. For the optical tweezer experiment,the important design criteria was the trade off between the overall DNA contour length that could be used with our setup and the percentage of sequence containing the above motif. To balance these diverging interests, we devised a sequence with a total length of 451bp. To ensure we do not dilute the effect of sequence, we duplicated the motif so that the sequence of interest constitutes more than half the total DNA length. Two symmetric lac operator sequences flank the motif duplicate and we intend to use them in future experiments.

3.2.2 DNA Constructs

The three designed constructs were cloned into plasmids by DNA 2.0. Using primers (MWG Biotech), modified at 5' ends by biotin for one strand and digoxigenin for the other, the constructs were PCR amplified using TAQ polymerase (NEB) and the amplified sequences extracted using gel purification kits from Promega.

3.2.3 Sample Preparation

Sample chambers were prepared by affixing a small parafilm spacer between a coverslip and a microscope slide. The chamber was flushed with Phosphate Buffered Saline (PBS,GIBCO) and then incubated with anti-digoxigenin (Roche Chemical) at a final concentration of 20ug/ml in PBS for an hour. After incubation with anti-digoxigenin, the chamber was coated with casein (3mg/ml) for 10 minutes to prevent non-specific adsorption of the DNA and/or the bead. Concurrently, the DNA sample was tumbled on a rotary mixer with 0.8um diameter streptavidin coated polystyrene beads (Spherotech). The Bead:DNA ratio was kept high to prevent binding of more than a single dsDNA strand to the same bead. The DNA-bead solution was flowed through the chamber after passivation and incubated for 5 minutes. Following this, the chamber was flushed with buffer containing casein to most of the excess beads.

3.2.4 Gel Mobility Assay

The DNA sequences were initially amplified with unmodified primers and roughly equal concentrations were prestained with Lonza Gel Star stain. These were then run on 4-20% precast polyacrylamide gels (Invitrogen) at 100V in Tris Borate EDTA (TBE) buffer using standard electrophoresis instruments and images were taken using a standard imager. Besides the three sequences, a control 100bp ladder was run alongside.

3.2.5 Computational Analysis

Trinucleotide curvature analysis was performed using consensus trinucleotide parameters [*Brukner et al.* (1995)]. DNA tools [*Vlahoviček et al.* (2003)] was used to generate the three dimensional PDB files. Comparisons as illustrated were done using PyMol. Various trinucleotide and dinucleotide parameters were obtained from different sources (given in 3.2) and consolidated using perl and shell scripts to perform

analysis for the sequences.

3.2.6 Force Extension Measurements

The description of the optical tweezers setup has been provided in an earlier paper [*Chen et al.* (2009a)] and was described in the previous chapter. For the axial tweezer measurement, the bead was trapped in the linear region of the optical trap where the optical force remains nearly constant and images of the bead were captured using a CCD camera. The radial intensity profile of the image was fit to a quadratic function that yields the apparent size of the bead. This apparent size linearly decreases with increasing distance between the coverslip and the bead and hence, the size of the bead can be used to determine the extension of the DNA on application of a force. The force was then varied in steps by controlling an Acousto-Optic Modulator to change the intensity of the laser beam using a custom Labview program. The axial position of the bead over 400 frames for every measurement was averaged.

3.3 Results

The design of the DNA construct is very crucial in delineating the effect of sequence on elasticity from the effects of curvature. The three designed constructs share an identical sequence modified with stretches of either AT/GC to vary the stiffness (figure 1). We have varied the sequences of constructs such that their curvature are similar. While there might be differences in local curvature within a helical length, the overall sequences have very similar curvatures. This similarity in curvature was verified using consensus trinucleotide parameters. Modeling the sequences using the BendIT program [*Vlahoviček et al.* (2003)] also suggested similarity between their structures. (figure 3.1)

Gel mobility assays were performed to confirm the absence of any difference in intrinsic curvature in the DNA sequence experimentally. The three 451bp sequences

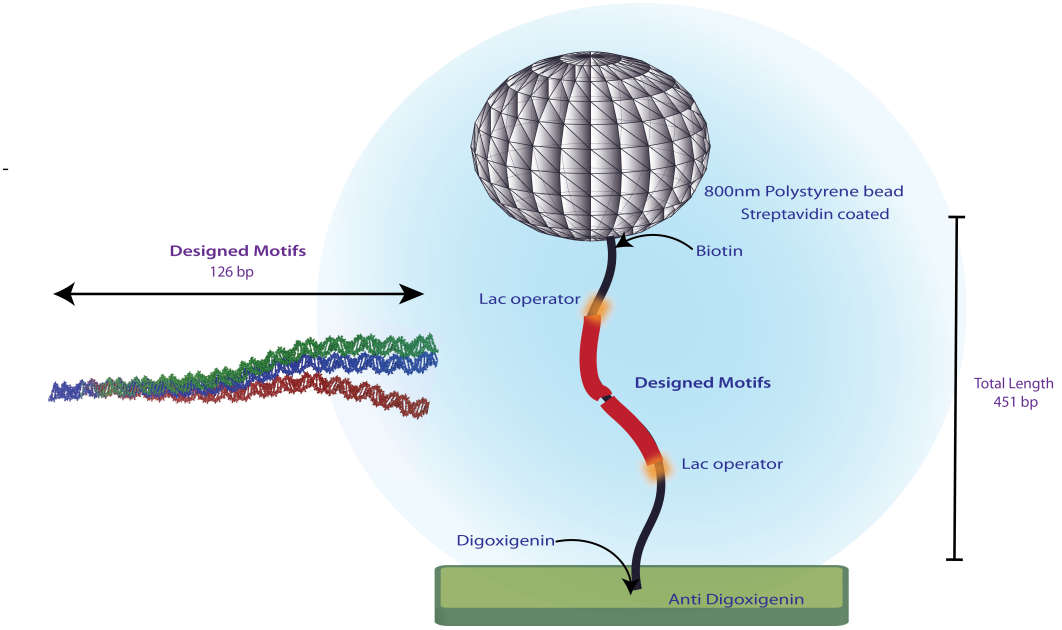

Figure 3.1: **Design of Sequences for Tweezers Experiment:** Three basal sequences were constructed (132bp length) having similar curvature but varied AT content. AT rich sequence is shown in red, the GC rich in green and control sequence is shown in blue. Three dimensional structure of th sequences shown here was generated by ModelIt software and rendered using Pymol. For stretching experiment, the basal sequences were duplicated and two lac operator sites and two random common sequences were added to either end of the duplicated basal sequence. Streptavidin coated polystyrene bead was tethered to the one of the construct end was coupled to the glass surface through digoxigenin/anti-digoxigenin linkers through primer modifications and subsequent PCR amplification.

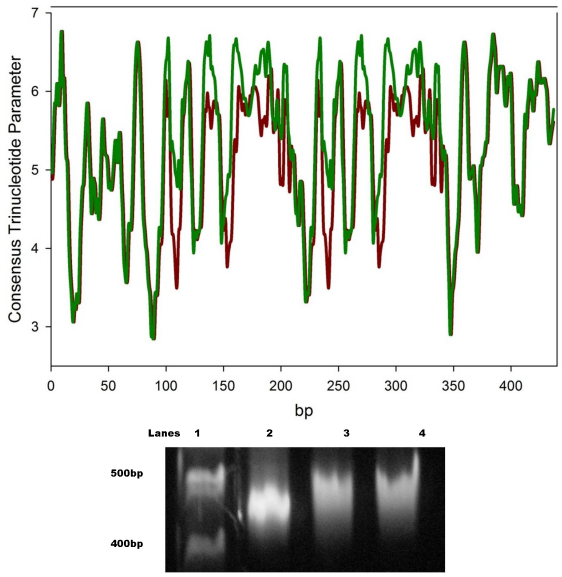

Figure 3.2: **Comparison of Curvature of Sequences:** (A)Consensus trinucleotide parameters were obtained from Brukner et al [*Brukner et al.* (1995)] and used to generate a running window average profile (10bp averaged) of the entire 451bp sequences. The results show that the curvature overlaps between the two sequences. (B) Polyacrylamide Gel Electrophoresis of the sequences run from top to bottom: Lane 1: 400 and 500bp of a 100bp ladder. Lane 2: AT rich sequence Lane 3: GC rich sequence Lane 4: Control sequence. The gel also shows similar migration between migration between the sequences suggesting similarity in curvature between the sequences

showed minimal variation in mobility when they were run on polyacrylamide gels as seen in figure 3.2. The sequences ran nearly midway between the 400bp and 500bp bands of the control 100bp ladder. This confirms our theoretical calculations that the three sequences have very similar curvature. To determine the unique role of sequence on elasticity, we then performed experiments with our constant force axial optical tweezers.

The elasticity of a short polymer can be quantified by its effective persistence length (l_p^*)*Geggier and Vologodskii* (2010). The effective persistence length depends on the length of the polymer, thereby differing from the conventionally used nominal persistence length (l_p). The nominal persistence length can be related to the effective

persistence length through an empirical equation 3.1 as determined by Seol et al [*Seol et al.* (2007)] and verified by our group [*Chen et al.* (2009a)]

$$l_p^* = \frac{l_{p\infty}}{1 + \frac{2.78 l_{p\infty}}{L}} \tag{3.1}$$

where L is the contour length of the DNA.

For short lengths of DNA, the effects of curvature and elasticity are not averaged out and thus the effective persistence length can vary from the mean value. The effective persistence length of a DNA sequence can be determined from stretching experiments using our constant force optical tweezers. Detailed description of the tweezers setup and its calibration have been described in our previous paper [*Chen et al.* (2009a)].

Force extension curves of the three sequences used in our experiments are shown in figure 3.3. This force extension data was then fitted to a modified Worm Like Chain model to determine the effective persistence length of the DNA

$$F_{OPT} = F_{WLC}(x_o + x_{opt}, l_p^*, L) - F_{WLC}(x_o, l_p^*, L) \tag{3.2}$$

where F_{OPT} is the optical force, x_{opt} is the extension of the DNA on applying the optical force and x_o is the extension in the absence of an external force and accounts for the excluded volume effects from the microsphere [*Seol et al.* (2007)]. F_{WLC} is determined by the standard Worm-Like chain model defined as

$$F_{WLC} = \frac{k_b T}{l_p^*} \left[\frac{1}{4(1-\epsilon)^2} - \frac{1}{4} + \epsilon \right] \tag{3.3}$$

where ϵ is the relative DNA extension.

For a contour length (L) of 451bp and a nominal persistence length ($l_p\infty$) of 51 nm, the effective persistence length of a typical sequence with 50% AT content is expected to be 26.73 nm. Our control sequence had an effective persistence length of

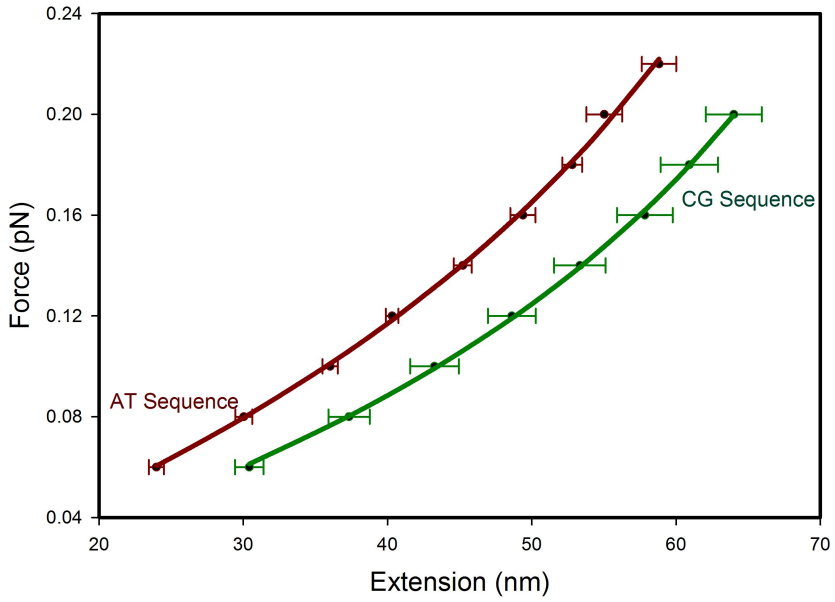

Figure 3.3: **Force Extension Curves :** Shown are two force extension curves, one for the AT rich sequence (red) and other for the GC sequence (green). The data for force extension measuremnts was taken from 9 datasets for AT rich sequence and from 7 for GC rich sequence. The values were then fitted using a modified Worm-Like Chain model to obtain the effective persistence length

27 nm which is in accordance with both theoretical model and our prior results. The measured effective persistence length of the other two sequence differs from the control sequence by 15%. To obtain a length independent nominal persistence length for our sequence, the percentage difference between its effective persistence length compared to the effective persistence length of a typical sequence should be multiplied with the nominal persistence length of long B-DNA. This gives a persistence length of 44.10 nm for the AT sequence and 58nm for the GC sequence. It must also be noted that the zero force extension of the sequences are similar.

Sequence	AT content	Effective l_p	Zero Force Extension	Nominal l_p
ATA/TAT	61	21.98(1.58)	22.06(4.40)	44
CGC/GCG	45	33.33(2.30)	23.96(5.35)	59
Control	49	26	27.17	50

Table 3.1: Results from Tweezer Experiment

3.4 Discussion

In our current work, the contribution of sequence specific DNA elasticity to the overall persistence length from that of curvature has been successfully isolated.For this, a methodology for designing sequences with similar curvature but varying base composition has been developed. This methodology was then used to design three sequences with increasing AT content.Force extension measurements performed on these sequences using a constant force axial optical tweezer was used to understand the differences in the mechanical properties of DNA due to sequence variability. These sequence variations were found to alter the elasticity of DNA significantly with the AT rich sequence having an effective persistence length 30% lower than the GC rich sequence. This is a departure from conventional dinucleotide and trinucleotide models which predict a much smaller change between the two sequences. [table 3.2] An important factor contributing to the discrepancy would be the inconsistencies in the

various models [*Scipioni et al.* (2002)] as parameters for elasticity may not be completely captured by the existing models.

Theoretical Calculated Property	ATA/TAT	CGC/GCG	Control
Nominal Persistence Length (Circularization Measurements) nm[1]	47.67	48.14	47.9
Nominal Persistence Length (Crystal Structure Data) nm [2]	39.95	51.28	47.49
Stacking Energy (dinucleotide modeling) kcalmol^{-1} [3]	-510.8	-559.2	-538.2
Interaction Energy (stacking and twisting) kcalmol^{-1} [4]	-6773.2	-6926.2	-6816
Bendability (Consensus) [5]	5.15	5.54	5.60
Bendability (DNAse I) [6]	5.87	5.54	5.60

Table 3.2: Comparison of Various Parameters (theoretical calculation)[1] *Geggier and Vologodskii* (2010) [2] *ME and RHTI* (1987) [3] *Protozanova et al.* (2004) [4] *Cooper et al.* (2008)[5] *Brukner et al.* (1995) [6] *Gabrielian et al.* (1996)

Comparison of theoretical predicted value for persistence length based on data from crystal structure concur with our results [*ME and RHTI* (1987)]. While the absolute values do not match our experimental results directly, the persistence lengths calculated from the crystal data and those experimentally determined for our sequence are merely shifted. The difference in persistence length of the two extreme sequences calculated from both these data is nearly 30% which is indicative of the inherent similarity in the results. Thus, our optical tweezers experiments are an effective methodology for determining stiffness parameters of short DNA constructs.

A different approach by Geggier and Vologodskii [*Geggier and Vologodskii* (2010)] can alternatively be used to obtain the persistence length for dinucleotides using ring circularization taking the curvature into account. However, our results deviate significantly from theirs. Geggier and Volgodskii's model predicts a theoretical persistence length of 47.8 and 48.2 nm respectively for our AT rich and GC rich sequence constructs while from our stretching experiments, the nominal persistence lengths are 44nm and 58nm for the same two sequences. Some of this discrepancy could be

attributed to the residual curvature present in the sequences used for constructing Vologodskii and Geggier's model. By complementing gel shift assays with the various modeling parameters, we have established a more rigid procedure for understanding the effects of sequence on elasticity while keeping the effects due to curvature minimal.

DNA has traditionally been considered as a semiflexible polymer, rigid under a persistence length. However, our results along with others, indicate that sequence modulated difference from elasticity can play a vital role in regulation especially in short stretches. There are several instances where the mechanical properties of DNA play a crucial role in biological function. The often quoted example of the nucleosome positioning code reflects the importance of sequence dependence of mechanical properties arising in local difference despite the overall homogeneities. Sequence inhomogeneities are also seen in the trypanosomal kinetoplast DNA which has a highly bent sequence. DNA curvature is also known to affect loop formation and consequently, the regulation of the genes like the lac operon. Similarly, promoter regions upstream of a gene are known to be AT rich and thus, flexible and are thought to play a crucial role in genetic regulation. Thus, both curvature and flexibility of DNA play a biologically vital role. Curvature has been well studied by various biophysical techniques at both bulk and single molecule level. However, as a consequence of the overlap of sequence effects of both curvature and flexibility, most existing models are definitive in predicting the effects of curvature but not sequence elasticity. For instance, structure based stiffness method predicts that the trinucleotide AAA/TTT is more flexible than CCC/GGG, while DNAseI bendability results predict the inverse results. Far from being an isolated example, there are other incompatibilties between the various models [*Gromiha* (2000)]. Some of these difficulty arise from not isolating the effect of flexibility from curvature and in general, delineating the importance of elasticity is still controversial and not adequately addressed.

Our experiments provide a solid methodology for separating the two effects, cur-

vature and elasticity. Our results show that the overall persistence length of DNA is sensitive to small variations in the sequence. This can have significant biological implications, as the need to bend DNA is a recurring theme in many cellular processes like packaging and looping. From our measurements, we found that the energetic cost of forming an AT rich loop is significantly lesser than the cost of bending a GC rich sequence. This difference in elasticity, is of consequence *in vivo*, where the cell can deftly utilize the elasticity of DNA in gene regulation.

3.5 Conclusions

In our earlier work, we had developed a constant force axial optical tweezer to understand the behavior of short DNA sequences. This work provides a platform to further explore sequence dependent parameters. Our current work establishes a methodology of separating elasticity from curvature and for understanding the effect of sequence on DNA flexibility. We have shown a strong dependence of persistence length on the sequence of DNA. The current work can be expanded to explore the entire gamut of sequence dependent elasticity parameters. We are performing further experiments to understand how gene regulation is directly affected by these sequences by following tethered particle motion of these sequences in the presence of lac repressor. This will be important in understanding the mechanical aspects of gene regulation.

CHAPTER IV

The Sequel : How does Elasticity Affect Looping?

4.1 Introduction

The previous chapter dealt with understanding the importance of sequence in modulating the mechanical behavior of DNA. A difference of 15% in AT content was shown to change the persistence length by almost 30%. The larger question remains as to how relevant these changes are in biological events. This chapter showcases the extent to which these differences in mechanical properties affect biological process. This chapter illustrates the importance of sequence dependent elasticity in regulating DNA-protein looping.

4.2 DNA Looping

DNA looping is a ubiquitous regulatory process found in all organisms [*Schleif* (1992)]. In fact, the canonical example of genetic regulation discovered by Jacob and Monod is the looping mediated by Lac repressor to modulate expression of the lactose operon [*Jacob and Monod* (1961)]. Experiments in the ensuing several decades have made this one of the most studied biological systems. The lactose repressor protein is a tetramer which binds to two sequences upstream of the genes forming a loop, preventing gene expression [*Friedman et al.* (1995)]. The thermodynamics and

kinetics of wild type lac operators have been investigated in a wide number of both single molecule and bulk experiments [*Fried and Crothers* (1981); *Hsieh and Brenowitz* (1997); *Frank et al.* (1997); *Han et al.* (2009)]. Further, looping also provides a platform for understanding novel experimental methods to follow DNA looping. Lac repressor looping has also been used extensively in understanding properties of DNA such as curvature and helical repeats. We have previously developed a TIRF-TPM method for looking at kinetics of DNA loops [*Blumberg et al.* (2005)]. We are currently working on how synthetic prebent DNA constructs loop and if curvature/phasing in sequences influences its looping rate.

It is very important to understand from a cellualar viewpoint, that there is fundamental difference between repression and looping and most *in vitro* assay look at DNA looping. For instance in the case of lac repressor, DNA stays in the looped state only on the order of hundred of seconds *in vitro*, but the repression of the lac operon *in vivo* can be completely blocked over generations [*Finzi and Dunlap* (2010)]. The gamut of experiments used to follow looping and repression are distinct at the moment [*Bond et al.* (2010)]. For instance, biochemical experiments that have been used to characterize repression cannot distinguish looped state from unlooped state. It is however, not difficult to envision an optical tweezer experiment that can look at RNA polymerase motion, while simultaneously looking at DNA tether length, like a single molecule version of minicircle transcription assay [*Lionberger and Meyhfer* (2010)]. Irrespective of the distinction between the two, the formation of a DNA loop remains the principal facet of repression. Understanding how the physical properties of DNA forming the loop affect looping kinetics will enable in gaining insights into gene repression.

Importance of the relationship between mechanics and looping rate can also help in answering questions like flexibility of nucleosomal sequence, as it is known that nucleosomal sequences have a greater tendency to loop (Rob Philips, unpublished).

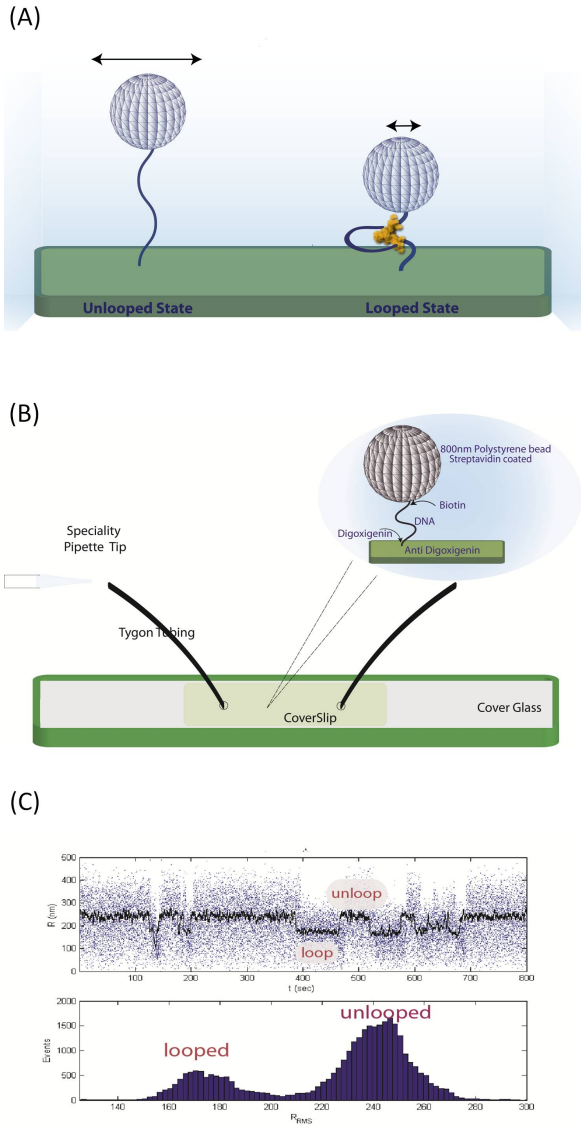

Figure 4.1: **Overview of Tethered Particle Motion:** (A) Principle : Upon binding of the protein, the tether length shortens and thereby the RMSD motion changes which can be seen in the time trace.(B) A cartoon representation of the chamber construction (C) This shows a representative data. The R values are plotted for all times and can be seen to be alternating between two states, looped which is shorter and unlooped which is longer. Life times of each state can now be determined and kinetic rates of the reaction can be determined.

Looping rates can enable in determining J-factors of short DNA sequences. Thus, looping of short DNA stretches can help us directly in understanding further DNA-protein interactions like in histones or centromeres.

4.3 Tethered Particle Motion(TPM)

A simple method for following DNA-protein looping kinetics is TPM. TPM has been used extensively in several single molecule studies to follow DNA-protein interactions [*Han et al.* (2009); *Towles et al.* (2009)]. The experiment is relatively simple and easy to carry out. The fundamental premise of TPM is that there is difference in effective contour length when the DNA loops [reviewed in *Finzi* (2009)]. By visualizing the XY Brownian motion of a bead tethered to one end of the DNA attached to a coverslip, the difference in contour length can be translated into difference in the extent of Brownian wiggles of the bead. This is further illustrated in figure 4.1. An advantage of a TPM experiment is that the theoretical timescale of observation is very high. Looping and unlooping lifetimes can be in the order of hours. Thus, it is possible to get precise looping/unlooping kinetics. We have carried out TPM experiments on the constructs mentioned in the previous chapter to understand how the difference in persistence length translates to difference in the lifetimes of loops. This enables us to understand the biological importance of elasticity of DNA.

4.4 Materials and Methods

4.4.1 DNA Constructs

The DNA sequences used in TPM experiments are exactly identical to the optical tweezers. The sequences had been designed to have two lac operator sites on either end of the constructed motif. The sequences are PCRed with primers modified with biotin and digoxigenin. A similar sample preparation as discussed previously in III is

used for TPM experiments.

4.4.2 Sample Preparation

A glass chamber was initially flushed with 200 μl of phosphate buffer saline solution (PBS). It was then incubated with 20 μg/ml (final concentration, in PBS) of anti-digoxigenin for an hour. To prevent non-specific binding of the polystyrene bead, the chamber was then incubated with 100 μl of PTC buffer (20 mM Tris-Acetate, pH 8.0, 130 mM KCl, 4 mM MgCl2 , 0.1 mM EDTA, 0.1 mM DTT, 20 μg/ml BSA, 80 μg/ml Heparin, 1 mg/ml α-casein) for 15 minutes. In tandem, 0.44um streptavidin coated microspheres and the sample DNA were incubated for 60 minutes on a rotating rack. The DNA:Bead concentration is such that there is excess bead so as to avoid double tethering. The concentration is diluted to have the apt number of beads while imaging. This mixture is subsequently added to the chamber and incubated for 15 minutes. After this, the chamber is washed with PTC buffer thrice. Following this, 200 μl LBB buffer(10 mM Tris-HCl, pH 7.4, 200 mM KCl, 0.1 mM EDTA, 1 mg/ml a-casein, 0.05 v/v DMSO, 0.2 mM DTT) is then flowed through the chamber, followed by 30 μl of LacI protein(a 200 pM final concentration) in LBB buffer. The sample is then imaged.

4.4.3 Imaging Methods

The tethered particles are imaged on brightfield microscope with a 1003 Olympus UPlan-FLN (oil, N.A. 0.61.3) objective. Images were taken on a Pixellink PL-B741(U/F) camera taken at around 30 frames per second. However, due to buffer overfill, there can be considerable drop in framerate which was subsequently taken into account for analysis. 1000 seconds of data was taken and the raw images stored as jpeg files.

4.4.4 Image Analysis

After imaging, the particles were tracked using a custom MATLAB script previously developed in our lab [*Milstein et al.* (2011)]. Briefly, the program tracked individual particles and the centre of the beads were determined using a Gaussian localization algorithm. The centre can be localized to an error of 5nm. The spatial coordinates thus determined were further Butterworth filtered (0.05 Hz) and the resulting data was free of slow drift. The spatial coordinates are then transformed into RMSD values. The RMSD data is then averaged (∼1-2s) to determine the looped or unlooped state lifetimes. A typical trace of the data is shown in figure 4.1C. A visual analysis of the RMSD value of the XY motion, after setting a threshold gives the precise lifetimes in each data trace. Lifetimes were compiled for the various states and fitted to single exponentials to extract kinetic data of looping and unlooping.

4.5 Results and Discussion

Property	AT sequence	CG sequence	Control
AT content (%)	45	61	49
Persistence Length (nm)	21.98	33.33	26.36
k_u (s^{-1})	.026(.003)	.012(.002)	.005(.001)
k_l (s^{-1})	.045(.018)	.069(.026)	.036(.006)

Table 4.1: Results from TPM Experiment

We performed TPM experiments on the three constructs. The lifetime of either states was measured in seconds. The data was binned into histograms based on the number of datapoints and spread of the timepoints. In general, we found that lifetime of unlooped state was shorter than the lifetime of looped state. We modeled reactions as first order kinetics with rate constants as shown in the reaction below.

$$looping \underset{k_l}{\overset{k_u}{\rightleftharpoons}} unlooping$$

The cumulative probability plots of both the unlooped-looped and looped-unlooped transitions were plotted and fitted to single exponential curves. The various rate constants are shown in table 4.1.

4.5.1 Looping of DNA

We find that the looping rates of the three DNA constructs did not vary significantly across the sequences. This is indicative of our previously summarized differences between cyclization and stretching experiments. Looping of DNA is similar to cyclization and looping results in DNA structurally changing into a similar conformation as a circularized DNA. Thus, the lack of difference between looping rate constants can be attributed to the similarity in cyclization persitsence length between our constructs.

4.5.2 Unlooping of DNA

The unlooping of DNA unlike looping should be sensitive to the elasticity of DNA. However, we find a rather curious result. As expected, the CG rich sequence has a higher unlooping rate constant compared to the control DNA, but AT rich sequence which is the least stiff of the three also stays in the looped lifetime the shortest and has the highest unlooping rate constant. We believe this is attributable to the pressence of AT rich sequences which can very easily destablize the looping of DNA by mimicking the lac repressor binding site. We are currently carrying out experiments to verify the same.

4.6 Future Directions

In an earlier paper [*Wilson et al.* (2010)], we have developed a semi analytical model for calculating J-factor for DNA sequence which can take local stiffness into

account. It will be interesting to see how theoretical results from this compare with experimental results of TPM.

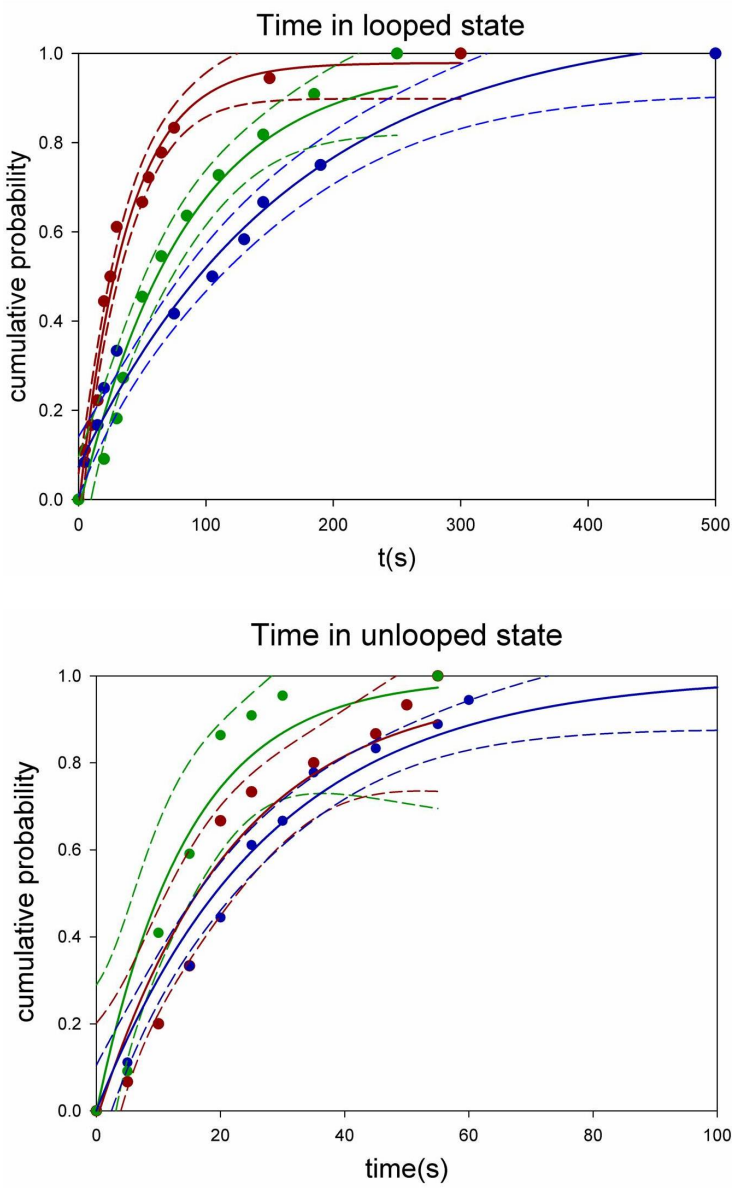

Figure 4.2: **Results-TPM:** The top figure is the fit to looped state lifetime while the bottom is the fit to time spent in unlooped state. The red is the AT sequence,the green is the GC rich sequence and blue the control sequence. The dashed lines represents the 95% confidence interval of the fit

CHAPTER V

Dungeons and Dicty: A Fluorescence Methodology to study DNA Dynamics inside a Cell

5.1 Introduction

Cells are brimming with molecular activity, but the cellular interior is much more than a test tube for biochemical reactions. The intracellular environment imposes a variety of mechanical constraints and engenders interactions both from molecular crowding to a range of motor-driven activity responsible for transcription, replication, cargo transport, cytoskeletal rearrangement, chromosomal remodeling and so on [*Milstein and Meiners* (2011)]. This host of activity gives rise to interactions between the DNA and its environment that go beyond purely passive thermal fluctuations, with broad implications for intracellular reaction kinetics and, ultimately, biological function. Already, significant effects from mechanical constraints and non-equilibrium fluctuations have been witnessed within the cytoplasm resulting in sub-diffusive behavior among elements embedded within the cytoskeletal matrix and super-thermal fluctuations apparent on long time scales [*Brangwynne et al.* (2008)]. However, these environmental effects are likely to differ substantially depending on the setting in which they occur, from the interior of prokaryotic bacteria to the nuclear compartment of eukaryotes, and the molecules they are acting upon, from the folding of

proteins to the protein-DNA complexes that control gene expression. It is, therefore, important to develop methods and techniques for assessing fluctuations as they act on specific macromolecules or biomolecular networks inside living cells.

A particularly interesting and biologically relevant process, where we would benefit from a clearer understanding of the effects of the cellular interior, is protein-mediated DNA looping [*Halford et al.* (2004)]. This common genetic motif allows for the communication of distant regulatory elements and the control of various transcription factors by a change in the topological conformation of the substrate DNA. In vitro assays, however, have found the rate of loop formation to be acutely sensitive to environmental fluctuations that interact with the DNA [*Chen et al.* (2010b)]. Unfortunately, a single-molecule method for observing the dynamics of this process in vivo is sorely lacking. The problem is that many regulatory DNA loops form on a spatial scale of less than 1 kbp along the DNA. At this length scale, individual fluorescent probes can no longer be resolved by fluorescence microscopy and methods like FRET become increasingly difficult due to the spatial and angular constraints required by the attachment of donor and acceptor fluorophores, a weak signal and photobleaching stemming from continuous illumination over extended periods of observation.

A prospective candidate for observing DNA looping in live cells is multi-color fluorescence imaging. One would label and then track the two operator sites that pair during the formation of a regulatory DNA loop using two distinct fluorophores. Such a scheme is not subject to the usual resolution limitations of single-color imaging, but there are many unique challenges to using multi-color signals to determine the distance between flourophores that arise from chromatic aberrations and the inherent difficulties of highly accurate image registration. Although much recent progress has been made in addressing these issues [*Joo et al.* (2008); *Pertsinidis et al.* (2010)], an analysis of the dynamic temporal correlations between two fluorescent labels can readily overcome these difficulties. Double stranded DNA (dsDNA) is an intrinsi-

cally stiff polymer and, in the absence of mechanical tension, displays exponentially decaying correlations between the orientations of tangent vectors along its length. The characteristic length of the correlations is known as the persistence length l_p, a parameter that indicates the stiffness of the polymer. In vitro measurements of ds-DNA yield a persistence length of roughly 50 nm, or 150 bp, which implies that two fluorescent labels attached at separations below this length will be more correlated in their relative motion than labels attached at greater distances.

By taking advantage of this property, we can study dynamical events like the formation of a regulatory loop in the DNA probe as the loop effectively brings the end labels to within a persistence length of each other. The temporal correlations displayed by the motion of the probe reveal both the conformational dynamics of the DNA and the effects of the intracellular environment on the DNA. Other applications of this method could be to witness a variety of cellular processes, such as chromosomal rearrangement or DNA cleavage, so long as the correlated motion of the two labels is altered during the dynamics. Furthermore, comparisons between live and dead cells can reveal the importance of active phenomena such as molecular motor action in driving an underlying biological process like the assembly of DNA-protein complexes.

As a demonstration of our technique, we have shown that quantum-dot end-labeled DNA of various lengths (90, 150 and 200 bp), when transfected into cells of the amoeba Dictyostelium discoideum, display resolvable differences in the spatio-temporal correlation of the motion of the quantum dots, providing a measure for the length of the intervening DNA. We see profound differences between live and dead cells, indicating that fluctuations along the DNA are strongly coupled to active processes within the cell. These results not only set the stage for direct observations of DNA looping in vivo, but also provide a new tool to the single-molecule arsenal of techniques for witnessing dynamical processes that occur on spatial scales below the diffraction limit [*Dorner et al.* (1990)].

5.2 Dual-Color Quantum Dot Labeling of DNA

. Linear strands of dsDNA, biotinylated at both ends, were individually end-labeled with two different colored streptavidin coated quantum dots (QD). We utilized commercially available QDs (Invitrogen) that display a narrow emission spectrum at 605 nm and 655 nm. We used two methods to assure that the DNA constructs were doubly-labeled. For the 90 bp DNA, we purchased two complementary biotinylated oligonucleotides, of random sequence, and tumbled each strand separately with one of the QDs in Borate buffer. The sample was purified in a 2% agarose gel so that only singly-labeled DNA was present and was then extracted from the gel with Freeze'n Squeeze (Roche) spin columns. The two singly-labeled strands of ssDNA were then annealed to form a 90 bp doubly-labeled strand of dsDNA.

Since commercially available oligonucleotides are typically limited to around 100 bps in length, we prepared our two longer constructs (150 and 200 bp) by a different procedure. For each, we purchased two pairs of complementary sequences, but varying in length, such that each pair could be annealed leaving a biotinylated strand of dsDNA with a 20 bp overhang. The DNA was engineered so that the overhangs on each of the resulting dsDNA segments were complementary. The dsDNA segments were attached to the QDs and purified as previously described for the 90 bp construct. However, to form the final construct required a ligation step to connect the pair of strands and to close the photodiester bond. We should mention that we had originally tried a simpler method for generating longer strands of doubly-labeled dsDNA. That was by cleaving a linear strand of DNA at a convenient restriction site, attaching the quantum dots, and then ligating the two halves together, but this proved very inefficient due to the small sequence length and, typically, palindromic nature of the overhangs. Our poor results with this method led us to the somewhat more complex, yet straightforward, method we have described (see Supporting Information for sequence information and a detailed protocol).

While the QDs provide a much stronger signal and resilience to photobleaching than traditional fluorophores, they tend to blink on and off randomly. Blinking is a known issue with QDs that is thought to result from Auger recombination between extra charge carriers on the QD and excited electron-hole pairs. These events lead to a dark state that prevents the QD from photoluminescing until the nanocrystal is neutralized. Non-blinking QD nanocrystals have been synthesized by blending the semiconductor material between the core and the shell; unfortunately, such QDs are not readily available and also display some unusual spectral properties. Two approaches that lessen the extent of blinking, although not completely alleviating the problem, are to either increase the thickness of the semiconductor shell, thereby raising the band gap, or to bind thiol groups to the QD by introducing chemicals such as dithiothreitol , β-mercaptoethanol or β-mercaptoethylamine to the solution. Since we only had access to commercially available QDs and were interested in live cell imaging, neither of these options were available to us. We were able to take advantage of the blinking behavior to confirm that our DNA constructs were end-labeled with only a single QD, but overall the effect posed a hindrance to our dynamical measurements that we were not able to control for. Nonetheless, the strong signal that we received from each pair of QDs allowed us to capture continuous video signals, at rapid frame rates (40 fps), for minutes at a time.

5.3 Cell Culture and Sample Preparation

An axenic strain of the amoeba Dictyostelium discoideum, obtained through the dictyBase.org stock center, was grown in a liquid broth of HL5 medium at ambient temperature *Froquet et al.* (2008). Transfection of the nanoparticles into the amoeba was done by directly mixing the labeled construct with a 2-3 day old culture and incubating for a period of between 45-60 mins.Active processes driven by ATP were suppressed by killing the cells as follows: CCCP, at a 20 μ M final concentration, was

added to the culture and the experiment was performed within the hour. Addition of CCCP is known to immediately reduce ATP content, but should not otherwise damage the cells.

5.4 Dual-Color Fluorescence Microscopy

All specimens were imaged on an inverted Zeiss microscope with an Olympus 100x, NA 1.4 oil-immersion objective (see Figure 5.1). The QDs were excited by a 405 nm 100 mW diode laser (CrystaLaser) that was optically expanded, low-pass filtered and fed into the back of the microscope. Both QDs display a high extinction coefficient at 405 nm so were well excited by the illumination. To image the two emission channels we used a DualView (Photometrics) imaging apparatus that separated the two colors and projected them on different regions of the same CCD (see Fig. 1). Cells where located by darkfield microscopy; however, the white light illumination was switched off during the fluorescence measurements. All images were acquired at 40 fps on a Cascade 650 (Photometrics) low-noise CCD camera and the images where tracked with custom Matlab software. The resulting data was high-pass filtered with a Butterworth filter at 0.05 Hz to remove slow drift. All images in which at least one of the QDs is dark where dropped from further analysis.

5.5 Correlation Measure

We begin by defining the correlation function $G_(i,j)(\tau)$ between the spatial vectors $x_i(t), x_j(t)$ of particles i,j within a temporal window of length T_w:

$$G_(i,j)(\tau) = \int_0^{(T_w-\tau)} \langle x_i(t).x_j(t+\tau)\rangle \, \mathrm{d}t \tag{5.1}$$

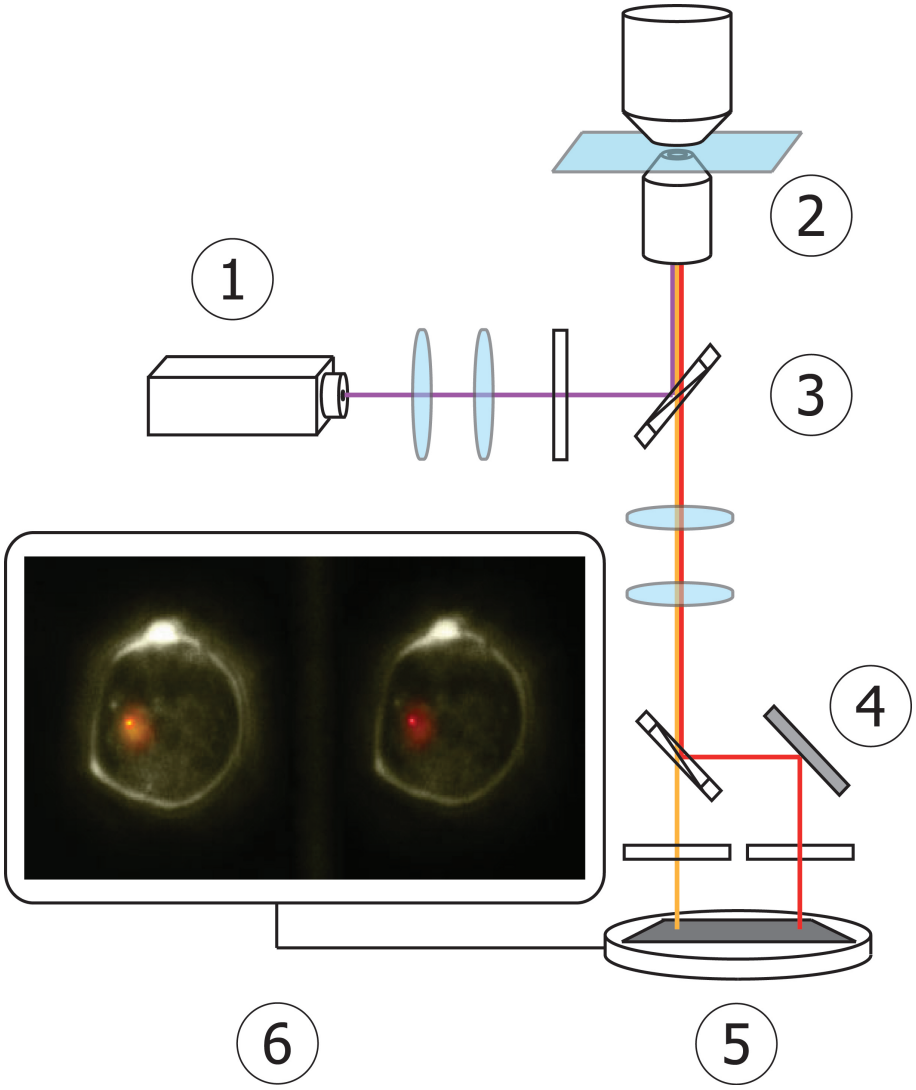

Figure 5.1: **Schematic of the Experimental Setup:** (1) 406 nm illumination laser for fluorescence; (2) 100x, 1.4 NA oil-immersion dark-field objective and custom mounted 1.1-1.5 NA dark-field condenser; (3) Inverted microscope with a 410 nm low-pass laser filter and a dichroic that cuts at 470 nm; (4) beamsplitter fitted with 605 nm and 655 nm bandpass filters and a dichroic that cuts at 630 nm; (5) cooled CCD camera. (6) False color image showing a D. discoideum cell that has ingested a double labeled construct. The picture was constructed by superimposing an image of the cell taken within dark-field mode with fluorescent imaging of the QD probes.

For example, for a 1-D freely diffusing object whose mean squared displacement ($MSD \propto t$), the normalized autocorrelation function (i.e., $i = j$) is simply $\frac{G(\tau)}{G(0)} = 1 - \frac{\tau}{T_w}$ We initially compared the autocorrelations $G_{1,1}(\tau), G_{2,2}(\tau)$ of the two fluorescent labels with the cross-correlation $G_{1,2}(\tau)$ reasoning that the cross-correlation should tend to zero as the tether length of intervening DNA increased. This analysis was, unfortunately, unable to consistently differentiate between constructs of varying lengths. An alternative, more sensitive approach, was found by transforming to CM, $R(t) = \frac{(x_1(t)+x_2(t))}{2}$, and relative, $r(t) = x_1(t) - x_2(t)$, coordinates. In this coordinate system, the CM primarily displays confined diffusive motion while the relative motion is more indicative of the length of the construct. For long tether lengths the relative and CM motion simply converge.

We analyze our data by creating a running time window in which we calculate the CM and relative autocorrelations. If the motion of the two fluorescent labels displays a higher degree of temporal correlations, the difference between the CM and relative autocorrelation curves should increase. Conversely, if the motion of the labels is not well correlated, the two curves should show more similarity to one another. To quantify this behavior we have defined the following measure:

$$\mu^2(t) = \frac{1}{N}\sum_{i=1}^{N}(G_R(\tau_i) - G_r(\tau_i))^2 \tag{5.2}$$

where $G_R(\tau_i)$ and $G_r(\tau_i)$ are the CM and relative autocorrelation functions at time-lag τ_i, which is similar to a least-squares measure of the difference between two curves. By comparing the autocorrelation curves at all allowable time lags, this analysis provides significantly more information than a comparison at zero time lag alone. While not exactly normalized, the higher the value of the correlation measure, for a given time window, the more correlated is the motion between the two labels.

Figure 5.2 shows the relative and CM autocorrelations for each of a 90 and 200 bp

construct. The plots were generated by dividing a 60 s run-time, collected at 40 fps, into 40 windows of 1.5 s each and averaging together the resulting autocorrelations. As the length of the construct increases, both the relative and CM autocorrelations approach one another, as expected. Equation 2 5.2 above provides a quantitative measure of this behavior and so, since we are interested in the temporal evolution of the correlations, we must address whether this measure provides a clear and distinct signal for constructs of differing lengths. Figure 5.3 shows that this measure is indeed sufficient to differentiate between our 90 bp and 200 bp constructs. However, this resolution is lost if we reduce the window size to below a second. By increasing the size of the running window to more than 1.5 s, we can again differentiate between the two constructs, this time with improved resolving power, but at the cost of temporal resolution.

5.6 Diffusion Confined within a Spherical Vacuole

From our data, it appears as if the end-labeled DNA gets internalized within vacuoles in the Amoeba, as opposed to the cytoplasm. This result was quite reproducible and was found for all Amoebas in which our labeled DNA was detected. A simple model for the CM motion of the labeled constructs within each vacuole is to assume that they participate in confined diffusion within a sphere of radius a [*Bickel* (2007)]. The diffusion equation can be solved in three-dimensions for the radial mean square displacement (MSD)$\langle \delta r^2(t) \rangle = \langle (r(t) - r(0))^2 \rangle$ as follows:

$$\left\langle \delta r^2(t) \right\rangle = \frac{6a^2}{5} - 12a^2 \sum_{n=1}^{\infty} \exp^{\left[-\beta_{1n}^2 \frac{t}{\tau_c}\right]} \frac{1}{\beta_{1n}^2(\beta_{1n}^2 - 2)} \tag{5.3}$$

which introduces the characteristic time $\tau_c = \frac{a^2}{D}$, with D the diffusion constant. The variables β_{1n} are the zeros of the derivatives of the spherical Bessel functions $j_1^{'}(\beta_{1n}) = 0$. In the long time limit, the MSD is given by $\langle \delta r^2(t) \rangle = \frac{6a^2}{5}$, which we

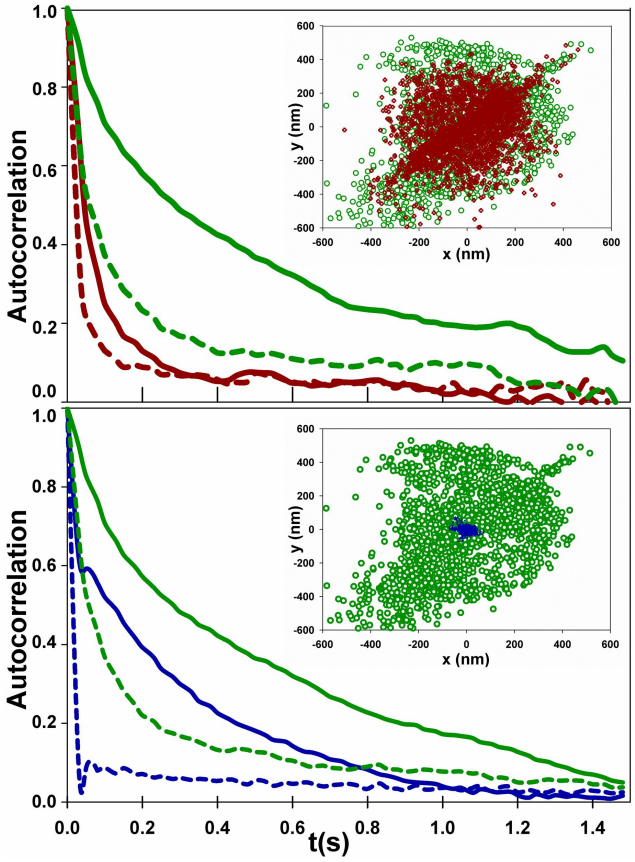

Figure 5.2: **Autocorrelation Funcion-CM and Relative:** The main figures show the CM (solid) and relative (dashed) autocorrelation functions within a window of 1.5 s and averaged over a 60 s acquisition time. The inserts show representative distributions of XY position from which the RMS distance can be computed and the size of the vacuoles inferred. (A.) Autocorrelation curves of 90 bp (green) and 200 bp (red) constructs. (B.) Autocorrelation curves of 90 bp constructs within living (green) and CCCP exposed (blue) cells.

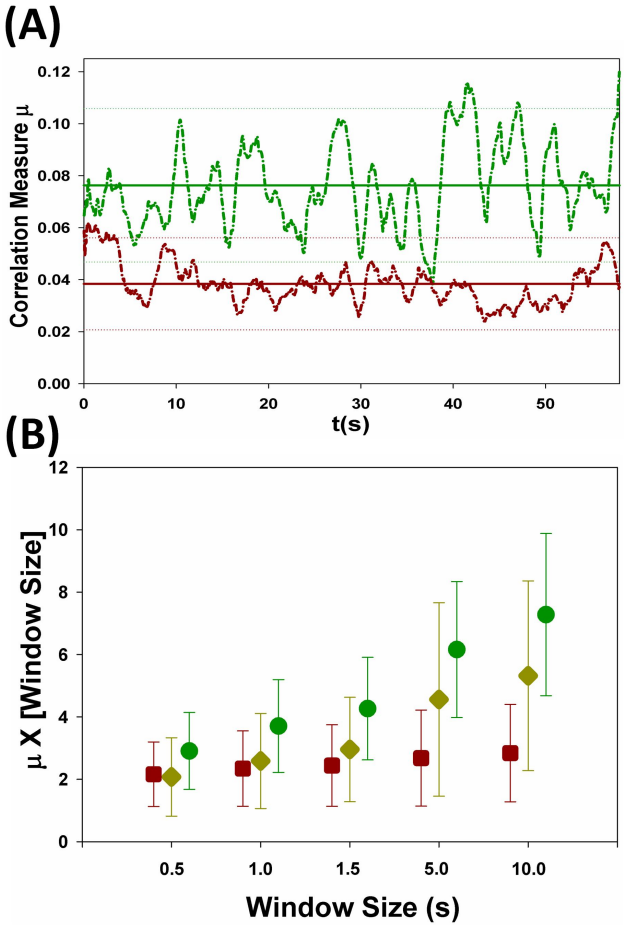

Figure 5.3: **Correlation Function as a Measure of DNA Length:** (A.) Correlation measure as a function of time calculated within a 1.5 s running window. The upper green (lower red) curve is for the 90 (200) bp construct. The solid lines give the mean of each curve and the dotted lines provide error bars of one standard deviation. The two curves are clearly distinguishable and display a higher correlation measure for the stiff 90 bp construct than the more flexible 200 bp one. (B.) Scaled mean correlation measure as a function of window size for 90, 150, and 200 bp (square, diamond, circle) constructs. For larger windows the samples are better resolved at the cost of time resolution.

can use to back out the radius a from our data when properly scaled to account for the two-dimensional projection of the three-dimensional motion. Equation 3 can then be fit to the CM mean square displacement of our QD labeled DNA constructs to produce a value for the diffusion constant. Table 1 shows the results.

5.7 Conclusion

. Our measured diffusion coefficients of approximately $6x10^{-}14\frac{m^2}{s}$ for the two DNA quantum dot constructs is substantially smaller than the reported diffusion coefficients for single quantum dots [*Yum et al.* (2009)], or DNA [*Lukacs et al.* (2000)] injected into HeLa cells of $10^{-12}\frac{m^2}{s}$ and $1-2\times10-11\frac{m^2}{s}$, respectively. We attribute this difference to additional entanglements between the dumbbell-like construct and its gel-like cellular environment slowing down diffusion on the observable time scale. The effective radii ($\sqrt{MSD}$) of the confining spheres, 189 nm and 322 nm for the 200 bp and 90 bp constructs, respectively, are within the expected range, while the difference between the two numbers can be attributed to the larger size exclusion layer around the bigger construct.

Our data also show a striking difference between live and dead cells. The diffusion coefficient is reduced by two orders of magnitude and the size of the effective sphere explored by the construct has dropped by one order of magnitude. Such a remarkable and drastic change in diffusive properties must be explained by an equally dramatic change in the viscoelastic properties of the medium inside the endocytotic vesicle and its dynamic coupling to the DNA quantum dot constructs. The diffusion coefficient obtained from Eq. 5.3(see Figure 5.4) reflects largely the behavior on short length and time scales, which is driven by the fluctuations of the cellular environment. Poisoning the cell with an ionophore like CCCP essentially stops all ATP-driven motor action in the cell, leaving only thermal motion as a source of fluctuations. ATP-driven fluctuations in the cytoskeleton and cytoskeleton-like gels have been shown to be two

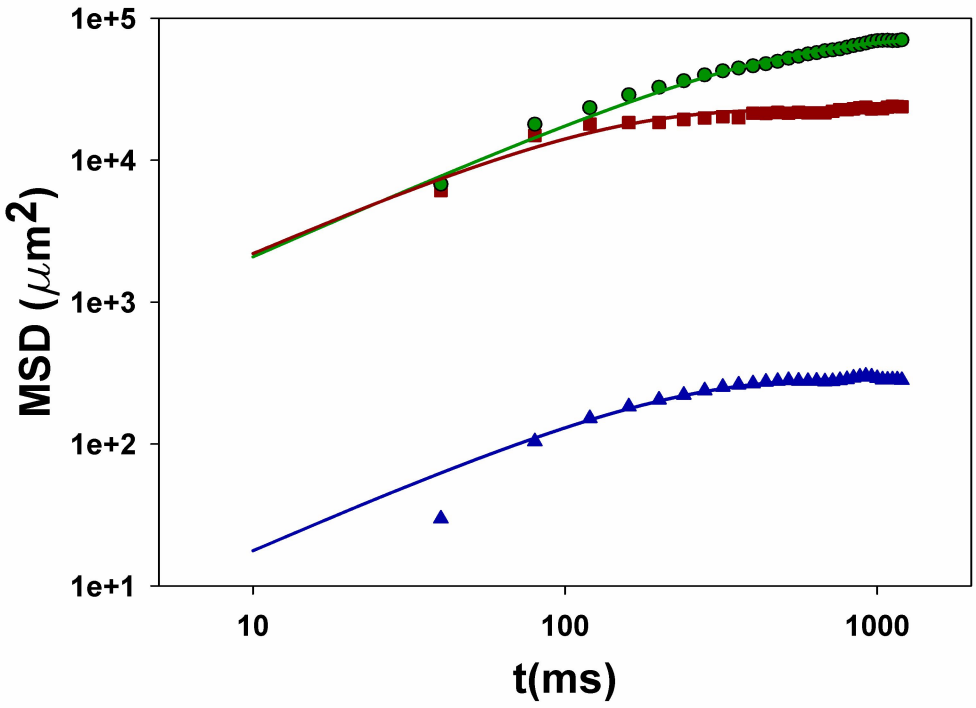

Figure 5.4: **Diffusion of DNA inside the Cell:** Center of mass (CM) mean square displacement (MSD) as a function of time for 90 bp (green) and 200 bp (red) constructs within living cells and for 90 bp constructs within CCCP exposed (blue)

orders of magnitudes stronger than thermal fluctuations on the hundred millisecond time scale [*Mizuno et al.* (2007); *Gallet et al.* (2009)], which is consistent with our results if we allow for a strong coupling of these athermal motions to our construct inside the endocytotic vesicle.

The plateau for the range of motion on long time scales corresponding to a strong confinement is more surprising. Shrinkage of the vesicle upon cell death to tens of nanometers, while not ruled out, appears unlikely. We are left to speculate that the viscoelastic properties of the medium in the vesicle have undergone a dramatic change. Our results imply that the absence of motor driven fluctuations does not merely reduce the effective temperature or enhance the viscosity since the constructs would

DNA construct	$\sqrt{(\overline{MSD})}$ (nm)	Diffusion Constant $\frac{m^2}{s}$
200bp	189	5.6×10^{-14}
90bp	322	5.9×10^{-14}
90bp(ATP depleted)	21	5.3×10^{-16}

Table 5.1: Root-mean-square motion of the doubly labeled constructs and the diffusion constants extracted from Fig. 4. For ATP depleted cells, the 90 bp constructs appeared to be much more confined and yielded a significantly smaller diffusion constant

still be able to explore the vesicle, albeit slower, and their MSD would asymptotically approach the value of the live cells. Rather, they tend to get stuck, as if they were in a solid that allows diffusive motion on short length and time scales, somewhat akin to a glass phase transition in driven granular media [*Jaeger et al.* (1996)].

Although our method could be employed to observe a variety of dynamic biological events, we have placed an emphasis on using it to witness DNA looping in vivo. For the moment, we have utilized large eukaryotic Amoeba cells, but many genetic circuits that are regulated by DNA looping events, such as the canonical lac operon, function within much smaller bacterial cells. For our method to work within such an environment, the QDs would have to be replaced with more traditional fluorophores. Replacing the CCD with a system of avalanche photodiodes could compensate for the diminished fluorescent signal, and allow for much faster acquisition rates, although the observation window would necessarily shrink due to the fluorescent instability of traditional fluorescent probes in relation to the QDs we currently employ. Nonetheless, the technique we have illustrated could serve as a powerful tool for witnessing biological dynamics at length scales that are quite difficult to observe if not wholly inaccessible to current single-molecule techniques.

CHAPTER VI

Back to the Roots: Constructing DNA Probes for Bacterial Systems

6.1 Introduction

While Dictyostelium was a great model for developing the *in vivo* DNA probe, it becomes imperative to work with bacterial systems for understanding looping. However, using a similar QD-label inside bacterial system is not feasible as QDs are large and cannot be ingested by bacteria. To overcome this, we need to design systems that can be used in bacterial system. Easiest would be to replace QD with a single flurophore. However, conventional organic fluorophores have low lifetimes and bleach easily. Hence, we need to label DNA with multiple fluorophores. In this chapter, construction of a dually labelled, multifluorophore system that can be used as a substitute for the QD labeled DNA is described.

6.2 Construct Design

The schematic for construction is shown in figure 6.1. Briefly, the two hairpin sequences differing by a restriction enzyme site were designed. Using fluorophore modified nucleotide, the hairpins were amplified and digested to leave an overhang which can be ligated with a linker DNA to get a closed labeled DNA.

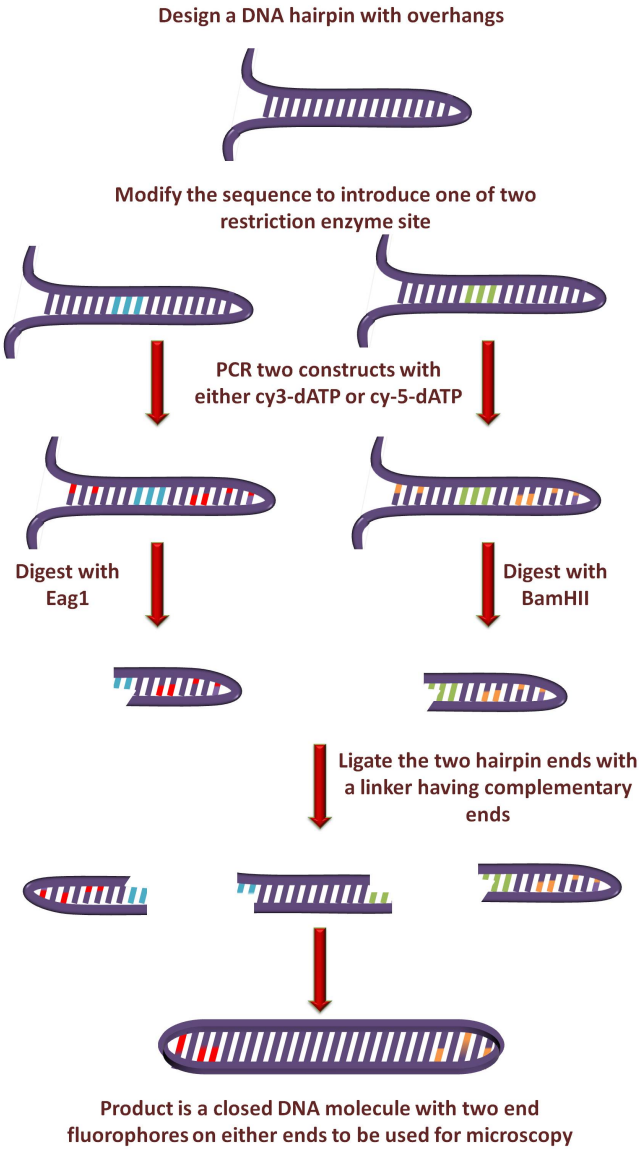

Figure 6.1: **Schematic of the Construct of a Two Color, Multiply Labeled Closed DNA Molecule:** Initially, we design a hairpin suitable for PCR having a overhang. Then we modify the sequence to have two different restriction enzyme sites, either EagI or BssHII . The enzymes are chosen such that there are no dA in it. The two sequences are then PCRed out with a nucleotide mix having modified dA. The dA are modified with either cy-3 or cy-5. The PCR mixture is then digested with the corresponding enzyme and this gives us two hairpins with overhangs. These hairpins are then ligated with a variable linker region which has complementary ends to both the hairpin overhangs. The final product is a two color, multiply labeled closed DNA molecule. Note: The BamHII should read as BssHII in the figure

6.2.1 Methods

Two 170bp DNA hairpin sequences (figure 6.2 A) were purchased from Biopioneer. The two sequences differ by 6 bases which correspond to sequences recognized by either EagI or by BssHII. Both these restriction enzymes recognize sequences not having an adenine. Hairpin structure of one of the sequences is shown in figure 6.2B. Two primers that are used, bind to the overhangs on either end and continue onto the hairpin. PCR was carried out as previously described by Kaur and Makrigiorgos [*Kaur and Makrigiorgos* (2003)].

PCR products were run on a 2% agarose gel and separated. Extraction from the gel was carried out using Quantum Freeze N Squeeze Prep from Biorad. PCR was found to work efficiently with and without labels. These are then digested with either BssHII or EagI enzyme. The digested hairpin has around 20 fluorophore labels. Following digestion, the products were immediately ligated using Quick Ligase. These were then coated on coverslips and imaged.

6.3 Dual View Imaging Setup

For imaging, we have modified the QD two color setup to include two different sources of illumination. (figure 6.3) A mercury lamp system which can simultaneously excite both cy3 and cy5 and a laser system which currently has a 640nm,100mW diode laser for exciting cy5, but can be readily expanded to include a 532nm laser for exciting cy3. However, before this system was built, the photobleaching experiments were performed in the Ari Gafni/Duncan Steel lab.

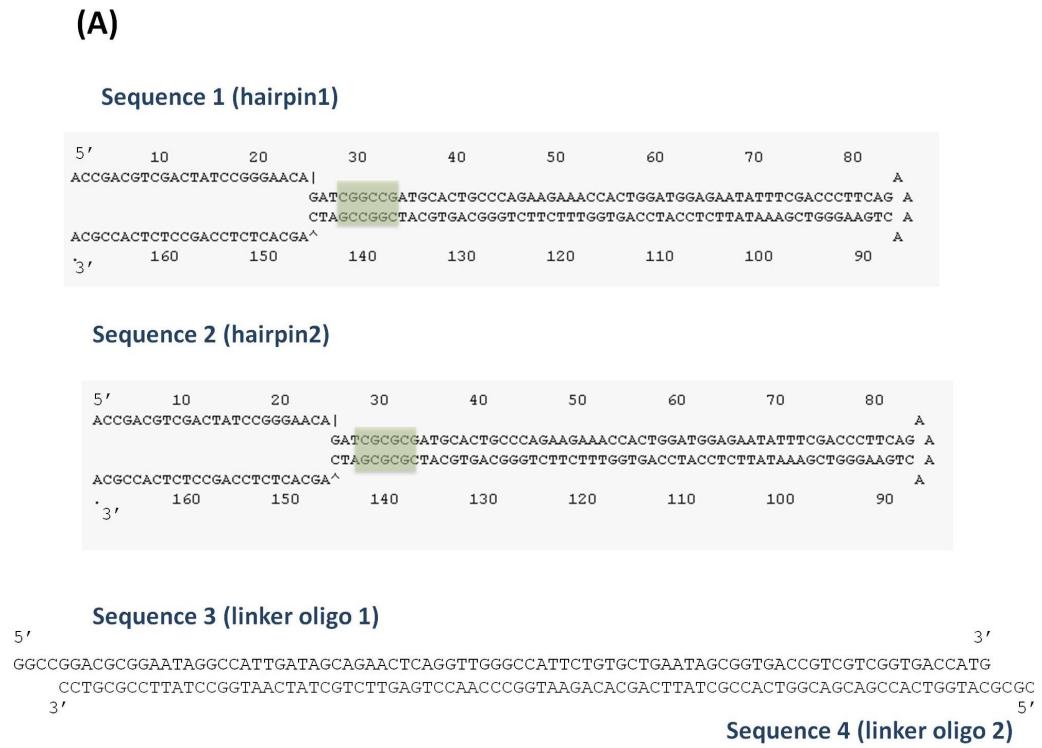

Figure 6.2: **Sequence Design:** (A) The figure shows the different sequences used. Sequence 1 and 2 are the two hairpins used. There are identical but for the restriction enzyme sites that are highlighted. The total size of the sequence is 170bp. Sequence 3 and Sequence 4 were purchased separately and annealed. Together they form the variable linker region. (B) We have verified computationally that the sequence forms a hairpin using MFOLD. The hairpin shown is the energetically favored structure.

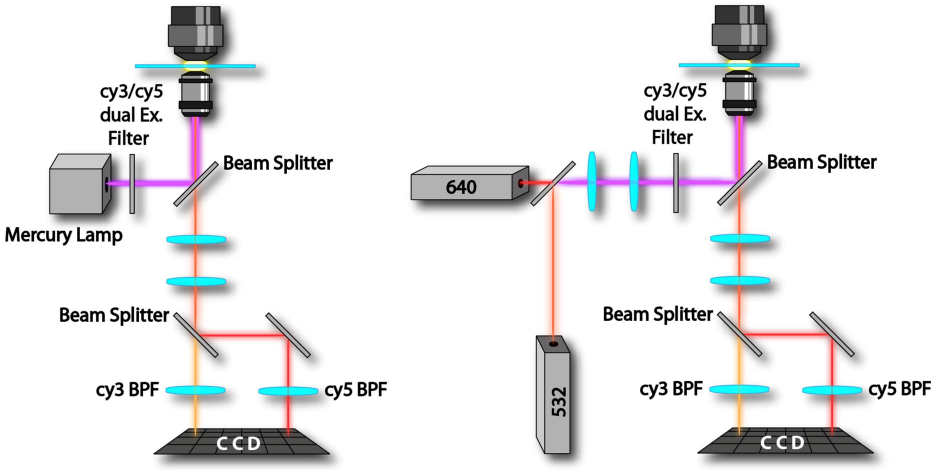

Figure 6.3: **Experimental Setup:** Schematic of the setup (left) The current setup which is similar to the setup used for previous chapter except the laser excitation is replaced with mercury lamp (100W) and appropriate filters are used. (right) The same modified with dual laser setup. The 640nm diode laser is in place and we will be adding the 532nm laser to the system.

6.4 Results

6.4.1 Verification of Multiply Labeled Hairpins

Hairpins were labeled with Cy-5 dyes as described previously and imaged using a TIRF microscope [*Ding et al.* (2009)]. The TIRF system is excited using a 640nm laser operating at 700uW power. A typical image is shown in figure 6.4 (inset). Aggregates of flurophores were avoided and a region having significant number of singular spots (no greater than two pixels) were imaged. Images were captured over time at 200ms exposure for 90s. Intensity of the individual spots were determined and temporally plotted. The photobleaching of several spots are shown in figure 6.4. The trajectories show a series of intensity drops indicating the bleaching of a fluorophore. Theoretically, it is possible to count the number of photobelaching steps so as to ascertain the number of fluorophores in a sample. However, for samples having a large number of fluorophores attached the sample of interest (greater than

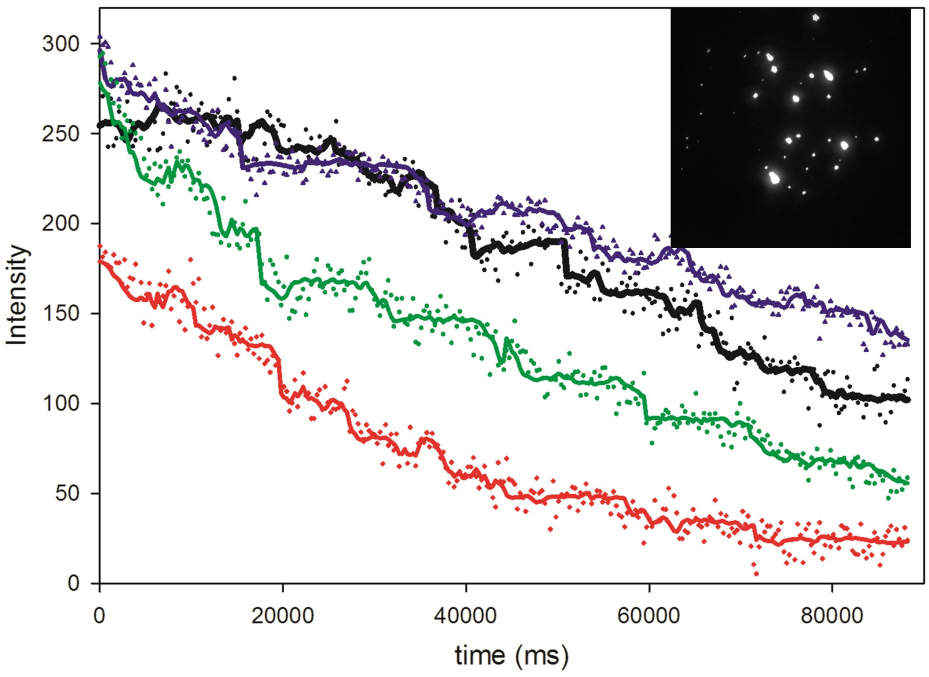

Figure 6.4: **Photobleaching of Hairpins:** Hairpins labeled with Cy-5 dyes were imaged using an EMCCD camera (inset). Images having clumps of fluorophores were avoided and fluorophores spanning 1-2 pixels were imaged. Photobleaching trajectories of hairpins are shown here

10-12 approximately), photobleaching steps are no longer explicit as is seen in our case (figure6.4). However, it is clear that we have hairpins multiply labeled and some of the photobleaching steps can be seen unambiguously. A more detailed discussion on photobleaching can be found here [*Ding* (2009)].

6.4.2 Using a Dual View System to View Hairpins

The photobleaching results were obtained using a TIRF system and a highly sensitive EMCCD camera. However, for visualizing two flurophores simulatenously, the two color system used for the previous QD experiments, should be modified for use with organic fluorophores. The 405nm diode laser was replaced with a 640nm diode laser (Cube) and an alternate illumination source, a mercury vapor arc lamp was used. The filters used for quantum dots were replaced with appropriate optics.

Figure 6.5: **Proof of Principle:** It is possible to image cy3/cy5 using our setup. Here, we are imaging cy3-hairpin coated on a coverslip.

As a proof of principle that of our system, a representative hairpin, Cy3 labeled is shown (figure 6.5). Our experiments show there is practically no bleed through to the Cy5 channel. Similar results were seen for the Cy5 hairpin too.

6.5 Current Outlook

Currently, we are working on constructing dually labeled constructs to simultaneously visualize both the dyes. We have successfully managed to ligate hairpins without fluorophores together. We are simultaneously trying to optimize conditions that can be used for ligating ends that have hairpins which we think will be similar to the hairpins without the fluorophores. The next step will be to introducing these into bacteria. We will be following standard transformation protocol with E. *coli* DH5α from Invitrogen and image it using the mercury lamp and two color dual view setup. This standardized procedure can then be used for multiple experiments and will be invaluable for studying dynamics of DNA inside bacteria.

APPENDICES

APPENDIX A

Supplementary - Optical Tweezer

A.1 Hydrodynamic Friction Coefficient

For determining the hydrodynamic friction coefficient of the microsphere near a surface one can use the following expansion:

$$\eta = 6\pi\eta r \frac{4\sinh\alpha}{3} \sum_{n=1}^{\infty} \frac{n(n+1)}{(2n-1)(2n+3)} \left[\frac{2\sinh(2n+1)\alpha + (2n+1)\sinh 2\alpha}{(2\sinh\frac{(n+1)\alpha}{2})^2 - [(2n+1)\sinh\alpha]^2} - 1 \right] \tag{A.1}$$

where the following shorthand has been introduced:

$$\alpha = \cosh^{-1}\frac{h}{r} = \log\left[\frac{h}{r} + ((\frac{h}{r})^2 - 1)^{\frac{1}{2}}\right] \tag{A.2}$$

The friction coefficient is defined in terms of the fluid viscosity η and the radius r of the microsphere, with the microsphere's center located a distance h above the surface. The summation converges reasonably well when expanded to about ten terms.

A.2 Modified Worm-Like Chain (WLC) model Influence of Axial Position on Stiffness Calibration

The calibration of the trap stiffness involves a tradeoff between the accuracy of the calibration, which increases with increasing distance from the surface, and the actual axial position where the trap is used experimentally. In general, the trap is calibrated at around 800-1000 nm from the surface, which is higher than the actual experimental condition.

A.3 Modified Worm-Like Chain (WLC) Model

The force extension curves can be fit to a modified WLC model that accounts for volume exclusion effects at zero optical force as follows:

$$F_{OPT} = F_{WLC}(x_o + x_{opt}, l_p^*, L) - F_{WLC}(x_o, l_p^*, L) \tag{A.3}$$

where F_{OPT} is the optical force, x_o is a fit parameter for the zero force extension, x_{opt} is the extension under force, L is the contour length of the DNA, and l_p^* is a second fit parameter for an effective persistence length. F_{WLC} is given by the usual WLC model

$$F_{WLC} = \frac{k_b T}{l_p^*}\left[\frac{1}{(4(1-\epsilon)^2)} - \frac{1}{4} + \epsilon\right], \tag{A.4}$$

where ϵ is the relative DNA extension. A more through discussion of the same can be found in *Chen et al.* (2009a).

APPENDIX B

Supplementary - *In Vivo* Experiments

B.1 Dual-Color Quantum Dot Labeling of DNA

We employed two methods to ensure that the DNA constructs were doubly-labeled. For the 90 bp DNA, we used two complementary biotinylated oligonucleotides of random sequence and incubated each strand separately on a rotating rack, at room temperature, with one of the QDs in Borate buffer. The sample was purified in a 2% agarose gel so that only singly-labeled DNA was present and was then extracted from the gel with Freezen Squeeze (Roche) spin columns. The two singly-labeled strands of ssDNA were then annealed to form 90 bp doubly-labeled dsDNA. A schematic of the same is shown in figure B.1.

Since commercially available oligonucleotides are typically limited to around 100 bps in length, we prepared our two longer constructs (150 and 200 bp) by a different procedure. For each, we purchased two pairs of complementary sequences, but varying in length, such that each pair could be annealed leaving a biotinylated strand of dsDNA with a 20 bp overhang. The DNA was engineered so that the overhangs on each of the resulting dsDNA segments were complementary. The dsDNA segments

were attached to the QDs and purified as previously described for the 90 bp construct. Then the final construct was formed by ligation to connect the pair of DNA segments and to close the photodiester bonds permanently. While the QDs provide a much stronger fluorescence signal and greater resilience to photobleaching than traditional fluorophores, they tend to blink on and off randomly. Blinking is a known issue with QDs that is thought to result from Auger recombination between extra charge carriers on the QD and excited electron-hole pairs2. These events lead to a dark state that prevents the QD from photoluminescing until the nanocrystal is neutralized. To lessen the extent of blinking one can bind thiol groups to the QD by introducing chemicals such as dithiothreitol , β-mercaptoethanol or β-mercaptoethylamine to the solution. Unfortunately, since we were interested in live cell imaging, these cannot be used and the blinking events cannot be avoided.

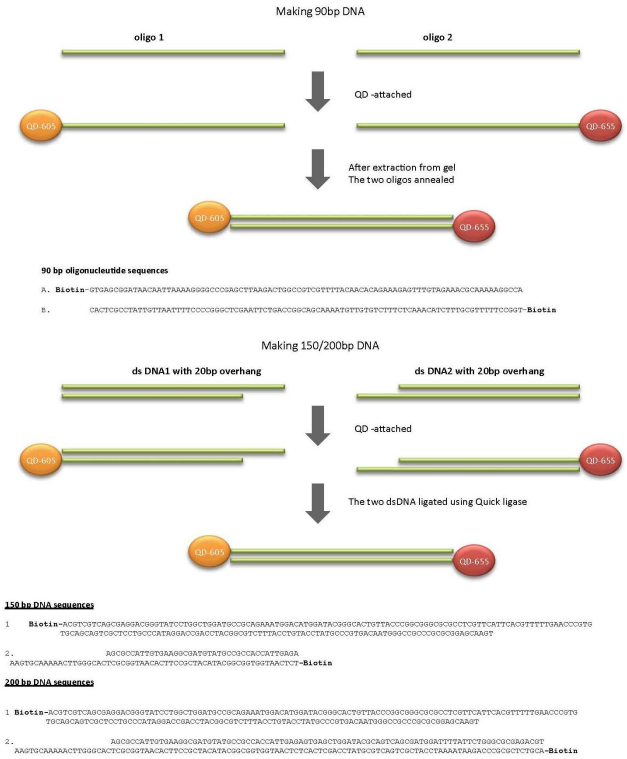

Figure B.1: **Schematic and Sequences of DNA:** (Top) Schematic figure of 90bp DNA construct and (bottom) corresponding oligonucleotide sequence. Schematic of 150/200bp DNA constructs and the corresponding oligonucleotide sequences

BIBLIOGRAPHY

BIBLIOGRAPHY

Adleman, L. M. (1994), Molecular computation of solutions to combinatorial problems, *Science*, *266*(5187), 1021–1024, doi:10.1126/science.7973651.

Allemand, J., S. Cocco, N. Douarche, and G. Lia (2006), Loops in DNA: an overview of experimental and theoretical approaches, *The European Physical Journal. E, Soft Matter*, *19*(3), 293–302, doi:10.1140/epje/i2005-10073-y, PMID: 16554978.

Baumann, G., R. F. Place, and Z. Foldes-Papp (2010), Meaningful interpretation of subdiffusive measurements in living cells (Crowded environment) by fluorescence fluctuation microscopy, *Current Pharmaceutical Biotechnology*, *11*(5), 527–543.

Becker, N. B., and R. Everaers (2007), From rigid base pairs to semiflexible polymers: Coarse-graining DNA, *Physical Review E*, *76*(2), 021,923.

Bickel, T. (2007), A note on confined diffusion, *Physica A: Statistical Mechanics and its Applications*, *377*(1), 24–32.

Blumberg, S. (2006), Disruptive effect of tension on protein-mediated DNA looping, Ph.D. thesis, University of Michigan, Ann Arbor.

Blumberg, S., A. Gajraj, M. W. Pennington, and J. Meiners (2005), Three-dimensional characterization of tethered microspheres by total internal reflection fluorescence microscopy, *Biophysical Journal*, *89*(2), 1272–1281.

Bond, L. M., J. P. Peters, N. A. Becker, J. D. Kahn, and L. J. Maher (2010), Gene repression by minimal lac loops in vivo, *Nucleic Acids Research*, *38*(22), 8072–8082, doi:10.1093/nar/gkq755.

Bouchiat, C., M. D. Wang, J. Allemand, T. Strick, S. M. Block, and V. Croquette (1999), Estimating the persistence length of a worm-like chain molecule from force-extension measurements., *Biophysical Journal*, *76*(1 Pt 1), 409–413, PMID: 9876152 PMCID: 1302529.

Brangwynne, C. P., F. C. MacKintosh, and D. A. Weitz (2007), Force fluctuations and polymerization dynamics of intracellular microtubules, *Proceedings of the National Academy of Sciences of the United States of America*, *104*(41), 16,128–16,133, doi:10.1073/pnas.0703094104, PMID: 17911265 PMCID: 2042173.

Brangwynne, C. P., G. H. Koenderink, F. C. MacKintosh, and D. A. Weitz (2008), Cytoplasmic diffusion: molecular motors mix it up, *The Journal of Cell Biology*, *183*(4), 583–587, doi:10.1083/jcb.200806149.

Brangwynne, C. P., G. H. Koenderink, F. C. MacKintosh, and D. A. Weitz (2009), Intracellular transport by active diffusion, *Trends in Cell Biology*, *19*(9), 423–427, doi:10.1016/j.tcb.2009.04.004.

Brukner, I., R. Sánchez, D. Suck, and S. Pongor (1995), Sequence-dependent bending propensity of DNA as revealed by DNase i: parameters for trinucleotides., *The EMBO Journal*, *14*(8), 1812–1818, PMID: 7737131 PMCID: 398274.

Calladine, C. R., and H. R. Drew (1986), Principles of sequence-dependent flexure of DNA, *Journal of Molecular Biology*, *192*(4), 907–918, PMID: 3586013.

Chen, Y., G. A. Blab, and J. Meiners (2009a), Stretching submicron biomolecules with Constant-Force axial optical tweezers, *Biophysical Journal*, *96*(11), 4701–4708, doi:10.1016/j.bpj.2009.03.009.

Chen, Y., D. P. Wilson, K. Raghunathan, and J. Meiners (2009b), Entropic boundary effects on the elasticity of short DNA molecules, *Physical Review E*, *80*(2), 020,903, doi:10.1103/PhysRevE.80.020903.

Chen, Y., J. N. Milstein, and J. Meiners (2010a), Femtonewton entropic forces can control the formation of Protein-Mediated DNA loops, *Physical Review Letters*, *104*(4), 048,301, doi:10.1103/PhysRevLett.104.048301.

Chen, Y., J. N. Milstein, and J. Meiners (2010b), Protein-Mediated DNA loop formation and breakdown in a fluctuating environment, *Physical Review Letters*, *104*(25), 258,103, doi:10.1103/PhysRevLett.104.258103.

Cloutier, T. E., and J. Widom (2004), Spontaneous sharp bending of double-stranded DNA, *Molecular Cell*, *14*(3), 355–362, PMID: 15125838.

Cloutier, T. E., and J. Widom (2005), DNA twisting flexibility and the formation of sharply looped proteinDNA complexes, *Proceedings of the National Academy of Sciences of the United States of America*, *102*(10), 3645–3650, doi:10.1073/pnas.0409059102.

Cooper, V. R., T. Thonhauser, A. Puzder, E. Schröder, B. I. Lundqvist, and D. C. Langreth (2008), Stacking interactions and the twist of dna, *Journal of the American Chemical Society*, *130*(4), 1304–1308, doi:10.1021/ja0761941.

Dauty, E., and A. S. Verkman (2005), Actin cytoskeleton as the principal determinant of Size-Dependent DNA mobility in cytoplasm a NEW BARRIER FOR NON-VIRAL GENE DELIVERY, *Journal of Biological Chemistry*, *280*(9), 7823–7828, doi:10.1074/jbc.M412374200.

DiGabriele, A. D., and T. A. Steitz (1993), A DNA dodecamer containing an adenine tract crystallizes in a unique lattice and exhibits a new bend, *Journal of Molecular Biology*, *231*(4), 1024–1039, doi:06/jmbi.1993.1349.

Ding, H. (2009), Single molecule studies of -amyloid (1-40) peptide in alzheimer's disease, Ph.D. thesis, University of Michigan, Ann Arbor.

Ding, H., P. T. Wong, E. L. Lee, A. Gafni, and D. G. Steel (2009), Determination of the oligomer size of amyloidogenic protein -amyloid(140) by single-molecule spectroscopy, *Biophysical Journal*, *97*(3), 912 – 921, doi:10.1016/j.bpj.2009.05.035.

Document, M. L. (2009), A detailed protocol for chamber construction and sample preparation can be found on our website.

Doi, M., and S. F. Edwards (1988), *The theory of polymer dynamics*, Oxford University Press.

Dorner, A. J., L. C. Wasley, and R. J. Kaufman (1990), Protein dissociation from GRP78 and secretion are blocked by depletion of cellular ATP levels, *Proceedings of the National Academy of Sciences of the United States of America*, *87*(19), 7429–7432, PMID: 2120699.

Du, Q., C. Smith, N. Shiffeldrim, M. Vologodskaia, and A. Vologodskii (2005), Cyclization of short DNA fragments and bending fluctuations of the double helix, *Proceedings of the National Academy of Sciences of the United States of America*, *102*(15), 5397 –5402, doi:10.1073/pnas.0500983102.

Finzi, L. (2009), Perspectives on dna looping, in *Mathematics of DNA Structure, Function and Interactions*, *The IMA Volumes in Mathematics and its Applications*, vol. 150, edited by C. J. Benham, S. Harvey, W. K. Olson, D. W. Sumners, and D. Swigon, pp. 53–71, Springer New York.

Finzi, L., and D. D. Dunlap (2010), Single-Molecule approaches to structure, kinetics and thermodynamics of transcriptional regulatory nucleoprotein complexes, *Journal of Biological Chemistry*, doi:10.1074/jbc.R109.062612.

Frank, D. E., R. M. Saecker, J. P. Bond, M. W. Capp, O. V. Tsodikov, S. E. Melcher, M. M. Levandoski, and M. Record Jr (1997), Thermodynamics of the interactions of lac repressor with variants of the symmetric lac operator: effects of converting a consensus site to a non-specific site, *Journal of Molecular Biology*, *267*(5), 1186–1206, doi:10.1006/jmbi.1997.0920.

Fried, M., and D. M. Crothers (1981), Equilibria and kinetics of lac Repressor-Operator interactions by polyacrylamide gel electrophoresis, *Nucleic Acids Research*, *9*(23), 6505–6525, doi:10.1093/nar/9.23.6505.

Friedman, A. M., T. O. Fischmann, and T. A. Steitz (1995), Crystal structure of lac repressor core tetramer and its implications for DNA looping, *Science*, *268*(5218), 1721–1727, doi:10.1126/science.7792597.

Froquet, R., E. Lelong, A. Marchetti, and P. Cosson (2008), Dictyostelium discoideum: a model host to measure bacterial virulence, *Nature Protocols*, *4*(1), 25–30, doi:10.1038/nprot.2008.212.

Fuller, R. S., J. M. Kaguni, and A. Kornberg (1981), Enzymatic replication of the origin of the escherichia coli chromosome, *Proceedings of the National Academy of Sciences*, *78*(12), 7370–7374.

Gabrielian, A., A. Simoncsits, and S. Pongor (1996), Distribution of bending propensity in dna sequences, *FEBS Letters*, *393*(1), 124–130, doi:DOI: 10.1016/0014-5793(96)00837-X.

Gallet, F., D. Arcizet, P. Bohec, and A. Richert (2009), Power spectrum of out-of-equilibrium forces in living cells: amplitude and frequency dependence, *Soft Matter*, *5*(15), 2947–2953, doi:10.1039/B901311C.

Garcia, H. G., P. Grayson, L. Han, M. Inamdar, J. Kondev, P. C. Nelson, R. Phillips, J. Widom, and P. A. Wiggins (2007), Biological consequences of tightly bent DNA: the other life of a macromolecular celebrity, *Biopolymers*, *85*(2), 115–130, doi:10.1002/bip.20627, PMID: 17103419.

Geggier, S., and A. Vologodskii (2010), Sequence dependence of DNA bending rigidity, *Proceedings of the National Academy of Sciences*, *107*(35), 15,421 –15,426, doi:10.1073/pnas.1004809107.

Goodsell, D. S., and R. E. Dickerson (1994), Bending and curvature calculations in B-DNA., *Nucleic Acids Research*, *22*(24), 5497–5503, PMID: 7816643 PMCID: 332108.

Goyal, S., N. C. Perkins, and J. Meiners (2008), Resolving the sequence dependent stiffness of DNA using cyclization experiments and a computational rod model, *Journal of Computational and Nonlinear Dynamics*, *3*(1), 011,003–6.

Grima, R. (2010), Intrinsic biochemical noise in crowded intracellular conditions, *The Journal of Chemical Physics*, *132*(18), 185,102–185,102–9.

Gromiha, M. M. (2000), Structure based sequence dependent stiffness scale for trinucleotides : A direct method, *Journal of Biological Physics*, *26*, 43–50.

Halford, S. E., A. J. Welsh, and M. D. Szczelkun (2004), ENZYME-MEDIATED DNA LOOPING, *Annual Review of Biophysics and Biomolecular Structure*, *33*(1), 1–24, doi:10.1146/annurev.biophys.33.110502.132711.

Han, L., H. G. Garcia, S. Blumberg, K. B. Towles, J. F. Beausang, P. C. Nelson, and R. Phillips (2009), Concentration and length dependence of DNA looping in transcriptional regulation, *PLoS ONE*, *4*(5), e5621, doi:10.1371/journal.pone.0005621.

Howard, B. (1961), The slow motion of a sphere through a viscous fluid towards a plane surface, *Chemical Engineering Science*, *16*(34), 242–251, doi:10.1016/0009-2509(61)80035-3.

Hsieh, M., and M. Brenowitz (1997), Comparison of the DNA association kinetics of the lac repressor tetramer, its dimeric mutant LacI adi , and the native dimeric gal repressor, *Journal of Biological Chemistry*, *272*(35), 22,092–22,096, doi:10.1074/jbc.272.35.22092.

Jacob, F., and J. Monod (1961), Genetic regulatory mechanisms in the synthesis of proteins, *Journal of Molecular Biology*, *3*, 318–356, PMID: 13718526.

Jaeger, H. M., S. R. Nagel, and R. P. Behringer (1996), Granular solids, liquids, and gases, *Reviews of Modern Physics*, *68*(4), 1259–1273.

James K, B. (1997), DNA enzymes: New-found chemical reactivity, *Current Biology*, *7*(5), R286–R288, doi:10.1016/S0960-9822(06)00138-2.

Joo, C., H. Balci, Y. Ishitsuka, C. Buranachai, and T. Ha (2008), Advances in single-molecule fluorescence methods for molecular biology, *Annual Review of Biochemistry*, *77*, 51–76, doi:10.1146/annurev.biochem.77.070606.101543, PMID: 18412538.

Kahn, J. D., and D. M. Crothers (1992), Protein-Induced bending and DNA cyclization, *Proceedings of the National Academy of Sciences*, *89*(14), 6343–6347.

Kahn, J. D., E. Yun, and D. M. Crothers (1994), Detection of localized DNA flexibility, *, Published online: 10 March 1994; | doi:10.1038/368163a0*, *368*(6467), 163–166, doi:10.1038/368163a0.

Kaplan, N., et al. (2008), The DNA-encoded nucleosome organization of a eukaryotic genome, *Nature*, *458*(7236), 362–366, doi:10.1038/nature07667.

Kaur, M., and G. M. Makrigiorgos (2003), Novel amplification of DNA in a hairpin structure: towards a radical elimination of PCR errors from amplified DNA, *Nucleic Acids Research*, *31*(6), e26, PMID: 12626725.

Koch, S. J., A. Shundrovsky, B. C. Jantzen, and M. D. Wang (2002), Probing Protein-DNA interactions by unzipping a single DNA double helix, *Biophysical Journal*, *83*(2), 1098–1105, doi:10.1016/S0006-3495(02)75233-8.

Kornberg, A. (2000), Ten commandments: Lessons from the enzymology of DNA replication, *Journal of Bacteriology*, *182*(13), 3613–3618, PMID: 10850972 PMCID: 94528.

Kraemer, H., M. Niemller, M. Amouyal, B. Revet, B. von Wilcken-Bergmann, and B. Mller-Hill (1987), lac repressor forms loops with linear DNA carrying two suitably spaced lac operators., *The EMBO Journal*, *6*(5), 1481–1491, PMID: 3301328 PMCID: 553955.

Kraemer, H., M. Amouyal, A. Nordheim, and B. Mller-Hill (1988), DNA supercoiling changes the spacing requirement of two lac operators for DNA loop formation with lac repressor., *The EMBO Journal*, *7*(2), 547–556, PMID: 2835234 PMCID: 454353.

Kruithof, M., F. Chien, A. Routh, C. Logie, D. Rhodes, and J. v. Noort (2009), Single-molecule force spectroscopy reveals a highly compliant helical folding for the 30-nm chromatin fiber, *Nature Structural & Molecular Biology*, *16*(5), 534–540, doi:10.1038/nsmb.1590.

Lander, E. S., et al. (2001), Initial sequencing and analysis of the human genome, *Nature*, *409*(6822), 860–921, doi:10.1038/35057062.

Lehming, N., J. Sartorius, M. Niemller, G. Genenger, B. v Wilcken-Bergmann, and B. Mller-Hill (1987), The interaction of the recognition helix of lac repressor with lac operator., *The EMBO Journal*, *6*(10), 3145–3153, PMID: 2826131 PMCID: 553756.

Lia, G., D. Bensimon, V. Croquette, J. Allemand, D. Dunlap, D. E. A. Lewis, S. Adhya, and L. Finzi (2003), Supercoiling and denaturation in gal Repressor/Heat unstable nucleoid protein (HU)-Mediated DNA looping, *Proceedings of the National Academy of Sciences*, *100*(20), 11,373–11,377, doi:10.1073/pnas.2034851100.

Lionberger, T. A., and E. Meyhfer (2010), Bending the rules of transcriptional repression: Tightly looped DNA directly represses t7 RNA polymerase, *Biophysical Journal*, *99*(4), 1139–1148, doi:10.1016/j.bpj.2010.04.074.

Lukacs, G. L., P. Haggie, O. Seksek, D. Lechardeur, N. Freedman, and A. S. Verkman (2000), Size-dependent DNA mobility in cytoplasm and nucleus, *Journal of Biological Chemistry*, *275*(3), 1625–1629, doi:10.1074/jbc.275.3.1625.

MacKintosh, F. C., and C. F. Schmidt (2010), Active cellular materials, *Current Opinion in Cell Biology*, *22*(1), 29–35, doi:10.1016/j.ceb.2010.01.002.

Maddox, B. (2003), *Rosalind Franklin: the dark lady of DNA*, HarperCollins.

Maheshri, N., and E. K. OShea (2007), Living with noisy genes: How cells function reliably with inherent variability in gene expression, *Annual Review of Biophysics and Biomolecular Structure*, *36*(1), 413–434.

Marilley, M., A. Sanchez-Sevilla, and J. Rocca-Serra (2005), Fine mapping of inherent flexibility variation along DNA molecules: validation by atomic force microscopy (AFM) in buffer, *Molecular Genetics and Genomics: MGG*, *274*(6), 658–670, doi:10.1007/s00438-005-0058-8, PMID: 16261347.

Marko, J. F., and E. D. Siggia (1995a), Stretching dna, *Macromolecules*, *28*(26), 8759–8770, doi:10.1021/ma00130a008.

Marko, J. F., and E. D. Siggia (1995b), Stretching DNA, *Macromolecules*, *28*(26), 8759–8770, doi:10.1021/ma00130a008.

ME, H., and A. RHTI (1987), Importance of dna stiffness in protein dna binding specificity, *Nature*, *329*, 263–266.

Milstein, J. N., and J. C. Meiners (2011), On the role of DNA biomechanics in the regulation of gene expression, *Journal of The Royal Society Interface*, doi: 10.1098/rsif.2011.0371.

Milstein, J. N., Y. F. Chen, and J. C. Meiners (2011), Bead size effects on proteinmediated DNA looping in tetheredparticle motion experiments, *Biopolymers*, *95*(2), 144–150, doi:10.1002/bip.21547.

Mizuno, D., C. Tardin, C. F. Schmidt, and F. C. Mackintosh (2007), Nonequilibrium mechanics of active cytoskeletal networks, *Science (New York, N.Y.)*, *315*(5810), 370–373, doi:10.1126/science.1134404, PMID: 17234946.

Moffitt, J. R., Y. R. Chemla, S. B. Smith, and C. Bustamante (2008), Recent advances in optical tweezers, *Annual Review of Biochemistry*, *77*(1), 205–228, doi: 10.1146/annurev.biochem.77.043007.090225.

Morgan, M. A., K. Okamoto, J. D. Kahn, and D. S. English (2005), Single-Molecule spectroscopic determination of lac Repressor-DNA loop conformation, *Biophysical Journal*, *89*(4), 2588–2596, doi:10.1529/biophysj.105.067728.

Neuman, K. C., and S. M. Block (2004), Optical trapping, *Review of Scientific Instruments*, *75*(9), 2787–2809, doi:doi:10.1063/1.1785844.

Norris, M. G. S., and N. Malys (2011), What is the true enzyme kinetics in the biological system? an investigation of macromolecular crowding effect upon enzyme kinetics of glucose-6-phosphate dehydrogenase, *Biochemical and Biophysical Research Communications*, *405*(3), 388–392, doi:10.1016/j.bbrc.2011.01.037, PMID: 21237136.

Pertsinidis, A., Y. Zhang, and S. Chu (2010), Subnanometre single-molecule localization, registration and distance measurements, *Nature*, *466*(7306), 647–651, doi: 10.1038/nature09163, PMID: 20613725.

Protozanova, E., P. Yakovchuk, and M. D. Frank-Kamenetskii (2004), Stacked-unstacked equilibrium at the nick site of dna, *Journal of Molecular Biology*, *342*(3), 775–785, doi:DOI: 10.1016/j.jmb.2004.07.075.

Raghunathan, K., Y. Chen, J. Blaty, B. A. Juliar, J. Milstein, and J. Meiners (2011), Mechanics of DNA: sequence dependent elasticity, in *Optical Trapping and Optical Micromanipulation VIII, Kishan Dholakia; Gabriel C. Spalding, Editors, 80970C*, pp. 80,970C–80,970C–8, doi:10.1117/12.895297.

Rothemund, P. W. K. (2006), Folding DNA to create nanoscale shapes and patterns, *Nature*, *440*(7082), 297–302, doi:10.1038/nature04586.

Schleif, R. (1992), DNA looping, *Annual Review of Biochemistry*, *61*, 199–223, doi: 10.1146/annurev.bi.61.070192.001215, PMID: 1497310.

Scipioni, A., C. Anselmi, G. Zuccheri, B. Samori, and P. De Santis (2002), Sequence-dependent DNA curvature and flexibility from scanning force microscopy images, *Biophysical Journal*, *83*(5), 2408–2418, doi:10.1016/S0006-3495(02)75254-5, PMID: 12414677.

Segal, E., Y. Fondufe-Mittendorf, L. Chen, A. Th|[aring]|str|[ouml]|m, Y. Field, I. K. Moore, J. Z. Wang, and J. Widom (2006), A genomic code for nucleosome positioning, *Nature*, *442*(7104), 772–778, doi:10.1038/nature04979.

Sengupta, P., T. Jovanovic-Talisman, D. Skoko, M. Renz, S. L. Veatch, and J. Lippincott-Schwartz (2011), Probing protein heterogeneity in the plasma membrane using PALM and pair correlation analysis, *Nature Methods*, *8*(11), 969–975, doi:10.1038/nmeth.1704.

Seol, Y., J. Li, P. C. Nelson, T. T. Perkins, and M. Betterton (2007), Elasticity of short DNA molecules: Theory and experiment for contour lengths of 0.67 m, *Biophysical Journal*, *93*(12), 4360–4373, doi:10.1529/biophysj.107.112995.

Shin, J., and W. Sung (2012), Effects of static and temporally fluctuating tensions on semiflexible polymer looping, *The Journal of Chemical Physics*, *136*(4), 045,101–045,101–6.

Shore, D., J. Langowski, and R. L. Baldwin (1981), DNA flexibility studied by covalent closure of short fragments into circles, *Proceedings of the National Academy of Sciences*, *78*(8), 4833–4837.

Skinner, G. M., B. S. Kalafut, and K. Visscher (2011), Downstream DNA tension regulates the stability of the t7 RNA polymerase initiation complex, *Biophysical Journal*, *100*(4), 1034–1041, doi:10.1016/j.bpj.2010.11.092, PMID: 21320448 PMCID: 3037602.

Strick, T., J. Allemand, V. Croquette, and D. Bensimon (2000), Twisting and stretching single DNA molecules, *Progress in Biophysics and Molecular Biology*, *74*(12), 115–140, doi:10.1016/S0079-6107(00)00018-3.

Strong, M., and D. Eisenberg (2007), The protein network as a tool for finding novel drug targets, *Progress in Drug Research. Fortschritte Der Arzneimittelforschung. Progrs Des Recherches Pharmaceutiques*, *64*, 191, 193–215, PMID: 17195476.

Towles, K. B., J. F. Beausang, H. G. Garcia, R. Phillips, and P. C. Nelson (2009), First-principles calculation of DNA looping in tethered particle experiments, *Physical Biology*, *6*(2), 025,001, doi:10.1088/1478-3975/6/2/025001.

Travers, A. A., and J. M. T. Thompson (2004), An introduction to the mechanics of DNA, *Philosophical Transactions of the Royal Society of London. Series*

A: Mathematical, Physical and Engineering Sciences, *362*(1820), 1265–1279, doi:10.1098/rsta.2004.1392.

Venter, J. C., et al. (2001), The sequence of the human genome, *Science (New York, N.Y.)*, *291*(5507), 1304–1351, doi:10.1126/science.1058040, PMID: 11181995.

Vlahoviček, K., L. Kaján, and S. Pongor (2003), DNA analysis servers: plot.it, bend.it, model.it and IS, *Nucleic Acids Research*, *31*(13), 3686 –3687, doi:10.1093/nar/gkg559.

Wang, M. D., M. J. Schnitzer, H. Yin, R. Landick, J. Gelles, and S. M. Block (1998), Force and velocity measured for single molecules of RNA polymerase, *Science*, *282*(5390), 902–907, doi:10.1126/science.282.5390.902.

Watson, J. D. (2011), *The Double Helix: A Personal Account of the Discovery of the Structure of DNA*, Simon and Schuster.

Widom, J. (2001), Role of DNA sequence in nucleosome stability and dynamics, *Quarterly Reviews of Biophysics*, *34*(3), 269–324, PMID: 11838235.

Wilson, D. P., A. V. Tkachenko, and J. Meiners (2010), A generalized theory of DNA looping and cyclization, *EPL (Europhysics Letters)*, *89*(5), 58,005, doi:10.1209/0295-5075/89/58005.

Yum, K., S. Na, Y. Xiang, N. Wang, and M. Yu (2009), Mechanochemical delivery and dynamic tracking of fluorescent quantum dots in the cytoplasm and nucleus of living cells, *Nano Letters*, *9*(5), 2193–2198, doi:10.1021/nl901047u, PMID: 19366190.

Zhou, Z., et al. (2009), Crowded Cell-Like environment accelerates the nucleation step of amyloidogenic protein misfolding, *Journal of Biological Chemistry*, *284*(44), 30,148–30,158.